NOVA SCHOOL OF SCIENCE & TECHNOLOGY

CHEMISTRY DEPARTMENT

MARIA AMARAL CABRITA RAMALHÃO FORTUNATO

BSc in Chemical and Biochemical Engineering

RADIOLABELLED PD-L1 INHIBITOR MONOCLONAL ANTIBODIES: SYNTHESIS, CHARACTERIZATION AND VALIDATION

MASTER IN CHEMICAL AND BIOCHEMICAL ENGINEERING

Universidade NOVA de Lisboa

April, 2023

NOVA SCHOOL OF SCIENCE & TECHNOLOGY

CHEMISTRY DEPARTMENT

RADIOLABELLED PD-L1 INHIBITOR MONOCLONAL ANTIBODIES: SYNTHESIS, CHARACTERIZATION AND VALIDATION

MARIA AMARAL CABRITA RAMALHÃO FORTUNATO

BsC in Chemical and Biochemical Engineering

Adviser: Francisco Silva,
Researcher, Radiochemist
Fundação Champalimaud

Co-advisers: Ana Sofia Capacho,
Radiopharmacist,
Fundação Champalimaud

Júri:

Presidente: Mário Fernando José Eusébio
Professor Auxiliar, Departamento de Química, FCT-NOVA

Arguentes: Helena Luísa de Araújo Vieira,
Professora Auxiliar, Departamento de Química, FCT-NOVA

Orientador: Francisco França Silva
Radioquímico, Fundação Champalimaud

MASTER IN CHEMICAL AND BIOCHEMICAL ENGINEERING

Universidade NOVA de Lisboa
March, 2023

Radiolabelled PD-L1 Inhibitor Monoclonal antibodies: Synthesis, Characterization and Validation

ACKNOWLEDGEMENTS

First and foremost, I would like to thank my supervisor, the researcher Francisco Silva and my co-supervisor, the radiopharmacist Ana Sofia Capacho, from the Nuclear Medicine-Radiopharmacology - Service/Lab of *Fundação Champalimaud*, for all the guidance, availability and dedication that allowed this work to be possible.

I would also like to thank Professor Mário Eusébio, who accompanied me not only during this work but also through the last years of my academic path, and to his group who supported the Q-TOF Analysis.

In general, I thank *Fundação Champalimaud* institution for the way I was received and accompanied throughout these months, namely Francisco Oliveira and Durval Costa from the Nuclear Medicine-Radiopharmacotology – Service/Lab, Cátia Feliciano from the Operations Unit, Ana Filipa Dias and Ana Raquel Tomás from Molecular and Transgenic Tools Platform, and finally Raquel Lopes and Cristina João from Myeloma & Lymphoma Research Group.

I also thank the pharmaceutical services at Fundação Champalimaud for providing the MPDL3280A, and also to Genetech for providing the 6E11 through a material transfer agreement.

Finally, this work would not have been possible without my family. To my mother, father, and sisters, for all their support, comprehension and motivation given through all my academic path.

At last, I thank all the professors of the Chemistry Department and to my colleagues who inspired and accompanied me for all these years.

I dedicate this work to my parents and sisters, for all their incentive and support.

ABSTRACT

Monoclonal antibodies have great potential for the treatment of cancer through Immunotherapy. However, certain immunotherapies, like PD-L1 inhibitors, are dependent of specific biomolecule expression in tumour sites. Hence, biopsies followed by histochemistry are required, which are invasive and may be aggressive depending on the anatomical location of the tumour and not translate its anatomical-functional heterogeneity. In this regard, Nuclear Medicine imaging may provide alternative diagnostic means. Medically relevant radiometals have been utilized, such as the isotope ^{111}In- emitting ɣ radiation, suitable for SPECT (Single-Photon Emission Computed Tomography) imaging.

In this work, PD-L1 Inhibitor monoclonal antibodies, such as Atezolizumab (human) and its murine equivalent 6E11 were conjugated with a chelator DTPA which allowed to their labelling with the radionuclide ^{111}In. From the resulting complexes, *in vitro* stability studies were performed in cell mediums, indicating that both conjugates remained stable with the radionuclide after 48 h.

Flow cytometry and cellular uptake assays were also performed, resulting in high binding and cellular accumulation in high PD-L1 expressing cancer cells, which is indicative of the potential of these antibodies as imaging agents for PD-L1 expression.

RESUMO

Anticorpos monoclonais possuem um grande potencial para tratamento oncológico através de Imunoterapia. No entanto, alguns tipos de imunoterapia, tais como inibidores de PD-L1, são dependentes da expressão de biomoléculas específicas nos tumores. Assim, biópsias seguidas de histoquímica são necessárias, sendo estas invasivas e podendo ser agressivas, consoante a localização anatómica do tumor para além de não traduzir a sua heterogeneidade anátomo-funcional. Deste modo, a imagem em Medicina Nuclear pode providenciar métodos alternativos de diagnóstico. Radiometais clinicamente relevantes têm sido utilizados, tal como o isótopo ^{111}In- que emite radiação ɣ, utilizada em SPECT (Single-Photon Emission Computed Tomography).

Neste trabalho, anticorpos monoclonais inibidores de PD-L1, tais como o Atezolizumab (humano) e o seu equivalente murino 6E11 foram conjugados com o quelante DTPA, que permitiu as suas radiomarcações com o radionuclídeo ^{111}In. Dos complexos resultantes, estudos de estabilidade *in vitro* foram executados em meios celulares, indicando que ambos os conjugados se mantinham estáveis com o radionuclídeo após 48 h.

Citometria de fluxo e estudos de *uptake* celular foram também realizados, apresentando resultados que revelaram um elevado grau de ligação e acumulação celular em células cancerígenas com elevada expressão de PD-L1, o que é indicativo do potencial destes anticorpos como agentes de imagem para expressão de PD-L1.

CONTENTS

1 INTRODUCTION 1

1.1 Context 1

1.2 Motivation 3

1.3 Objetives 6

1.3.1 General aim 6

1.3.2 Specific aim 6

1.4 Document structure 6

2 STATE OF THE ART 9

2.1 Introduction 9

2.2 Immunotherapy in cancer 9

2.2.1 Monoclonal antibodies 11

2.3 Nuclear medicine 14

2.3.1 Molecular imaging 15

2.3.1.1 Radiolabelling 18

2.3.1.1.1 Chelation 18

3 MATERIALS AND METHODS 22

3.1 MPDL3280A and 6E11 purification and conjugation with a DTPA derivate 22

3.1.1 Excipient removal for MPDL3280A 22

3.1.2 Conjugation of DTPA to MPDL3280A and 6E11 22

3.1.3 Characterization of the conjugates 23

3.1.3.1 QTOF analysis 23

3.1.3.2 Determination of concentration using *Nanodrop* 23
3.2 Radiolabelling of MPDL3280A-DTPA and 6E11-DTPA…. 24
3.2.1 Radiolabelling of the conjugates 24
3.2.1.1 Radiolabelling procedure 24
3.2.1.2 Radiochemical yield 24
3.2.1.3 Purification of the radiolabelled conjugates 24
3.2.1.4 *In vitro* stability studies 25
3.3 Biological Evaluation Studies…. 25
3.3.1 Cell lines 25
3.3.2 Flow Cytometry 25
3.2.3 Cellular uptake assays 26
4 RESULTS' PRESENTATION AND DISCUSSION 27
4.1 Synthesis and characterization of DTPA-containg mAbs.. 27
4.1.1 Concentration of the conjugates 30
4.2 MPDL3280A-DTPA and 6E11-DTPA labelling with ^{111}In…. 31
4.2.1 Radiolabelling procedure 31
4.2.2 Purification of the radiolabelled conjugates 33
4.2.3 *In vitro* stability studies for ^{111}In-MPDL3280A-DTPA and ^{111}In-6E11-DTPA 33
4.3 Biological Evaluation Studies…. 34
4.3.1 Flow Cytometry 34
4.3.2 Cellular uptake studies 36
5 CONCLUSIONS AND FUTURE WORK 38
5.1 Future work…. 39

LIST OF FIGURES

1.1 — Scheme of immunotherapy for PD-1/PD-L1. ..... …..2
1.2 — Immunohistochemical analysis of PD-L1….. 4
1.3 — Imaging PD-L1 expression in subcutaneous CHO xenographs…….. 5
1.4 — Molecular structure of ^{111}In and the chelating agent DTPA (^{111}In-DTPA)... 6
2.1 — The major categories of Immunotherapy..... 10
2.2 — Illustration of PET and SPECT..... 16
2.3 — Structure of the conjugated NHS-MAG$_3$…..... 19
2.4 — DOTA chelator..... 20
2.5 — Structure of cyclic DTPA 21
2.6 — Scheme of p-SCN-Bn-CHX-A"-DTPA molecular structure…… 21
4.1 — Scheme of the reaction of conjugation of the mAb to DTPA..... 28
4.2 — Mass spectrum presenting the range of DTPA molecules attached to MPDL3280A. ... 28
4.3 — Mass spectrum presenting the range of DTPA molecules attached to 6E11..... 29
4.4 — Calibration curve for the samples the correspondent concentrations. 30
4.5 — Scheme of the reaction of radiolabelling of the mAb-DTPA with ^{111}In. 31
4.6 — Scheme of TLC layers of $^{111}InCl_3$ labelled mAb-DTPA, free $^{111}InCl_3$ and $^{111}InCl_3$ labelled mAb. 32
4.7 — MPDL3280A-DTPA radiolabelling yield after 1h, 24h and 48h in the three mediums..33
4.8 — 6E11-DTPA radiolabelling yield after 1h, 24h and 48h in the three mediums 34
4.9 — PD-L1 expression in human cell lines binded to: a) Protein BV711 (control), b) MPDL3280A, c)MPDL3280A-DTPA…….....35
4.10 — PD-L1 expression in murine cell lines binded to: a) Protein BV711 (control), b) mAb 6E11, c) 6E11-DTPA……. 35
4.11 — Cellular uptake of mAbs to cell lines..... 36

LIST OF TABLES

2.1— List of mAbs approved for therapy 11
2.2— List of Preclinical mAbs. 12
2.3— Tecentriq effectiveness for the correspondent tumors 13
2.4— 6E11 investigation results for the correspondent tumors……13
2.5— List of radionuclides used in nuclear medicine 11
2.6— Strength and weakness of the main available imaging modalities used in molecular imaging ……18
3.1— Concentrations of the MPDL3280A solutions 23
4.1 — Radiolabelling yield of the conjugate MPDL3280A-DTPA with the variations 1-3..... .32

ACRONYMS

ACT	Adoptive cell transfer.
ADC	Antibody-drug conjugate.
AEs	Adverse Events.
DOTA	2,2′,2″,2‴-(1,4,7,10-tetraazacyclododecane-1,4,7,10-tetrayl)teraaceticacid.
DTPA	Diethylenetriamine pentaacetate.
EDC	1-Ethyl-3(3-dimethylaminopropyl) carbodiimide Hydrochloride.
FDA	Food and Drug Administration.
ICI	Immune checkpoint inhibitors.
IgG1	Immunoglobulin G1.
iTLC	Instant Thin Layer Chromatography.
mAb	Monoclonal antibody.
MAG3	Mercaptoacetyltriglycine.
MBqs	Mega Becquerels.
MRI	Magnetic Resonance Imaging.
NHS	N-Hydroxyl succinimide.
PBS	Phosphate buffered saline.
PD-1	Programmed Cell Death 1.
PD-L1	Programmed Cell Death Ligand 1.
PET	Positron-Emission Tomography.
RT	Retention time.

SPECT	Single Photon-Emission Computed Tomography.
TIC	Total Ion current.

1

INTRODUCTION

1.1 Context

Cancer, or malignant tumors and neoplasms, are inclusive terms for a group of diseases where some of the body's cells grow uncontrollably beyond their usual boundaries, invading and affecting adjoining parts of the body and spreading to other organs. There are various types of cancers, with particular physiological and biological characteristics, hence, a faithful diagnosis is essential for appropriate and successful treatment as every cancer type requires a specific treatment [1–3].

Depending on the type and stage of the disease, patients may undergo a combination of therapeutic approaches, such as surgery with chemotherapy, radiation therapy, immunotherapy, targeted therapy or hormone therapy [4]. Among these treatments, immunotherapy has been showing promising results over the past few years. Immunotherapy principle is based on the inhibition of immune checkpoints ligand–receptor interactions, repealing the immune-suppression exerted by tumor cells, and as a consequence leading to the recognition and destruction of the tumor cells by the immune system [5–7]. Programmed Cell Death Protein 1 (PD-1) plays a vital role in inhibiting immune responses and promoting self-tolerance through modulating the activity of T-cells. Programmed Cell Death Ligand 1 (PD-L1) is a transmembrane protein that is considered to be a co-inhibitory factor of the immune response, combining with PD-1 to reduce the proliferation of PD-1 positive cells and induce apoptosis [8].

The patient's selection for immunotherapy not only predicts early responses but can also reduce side effects. Currently, the assessment of cancer immune checkpoints inhibitors expression, such as PD-1 and PD-L1, is acquired through biopsy followed by immunohistochemistry. However, these biopsies, are invasive and may be aggressive depending on the anatomical location of the tumor, as well as not translating its anatomical-functional heterogeneity, leading to flawed measurements.

Finding alternative methodologies that can provide a faithful assessment of these cancer immune checkpoints can play a pivotal role in the future of immunotherapy. In this regard, the combination of immunology and radiopharmacology has potential for the development of new diagnostic strategies. Whole-body PD-L1 expression assessment can be possible using nuclear medicine techniques, such as administering a radiolabelled monoclonal anti-PD-L1 antibody to patients and acquiring images with a gamma camera or a positron-emission tomography (PET) scanner [5, 9, 10].

Molecular imaging allows the non-invasive pathophysiological processes, which can inform proper decision-making in preclinical and clinical scenarios, which can help researchers accelerate the development of immune cell therapies, enhancing therapeutic efficacy and reducing adverse effects. Molecular imaging technologies have improved with the development of new contrast agents, imaging agents, ligands, and probes. Molecular imaging techniques, such as fluorescence imaging, bioluminescent imaging, computed tomography, MR imaging, ultrasound, single photon-emission computed tomography (SPECT), and positron-emission tomography (PET) can be used effectively to track stem cells and immune cells for cancer treatments [11–16].

Monoclonal antibodies (mAbs) can specifically target tumor-cell antigens, as shown in figure 1.1, which has led to their use in the delivery radioisotopes to tumor sites. Monoclonal antibodies can be labelled with specific radionuclides, depending on the radionuclide physical properties, and intended use. Using radiolabelled mAbs with imaging techniques, such as SPECT or PET provides critical data that are essential for predicting side effects as well as determining an optimal antibody dose and treatment. All the parameters obtained from these data are useful for guiding therapy responses, predicting toxicity and identifying patients most likely to benefit from treatment [17].

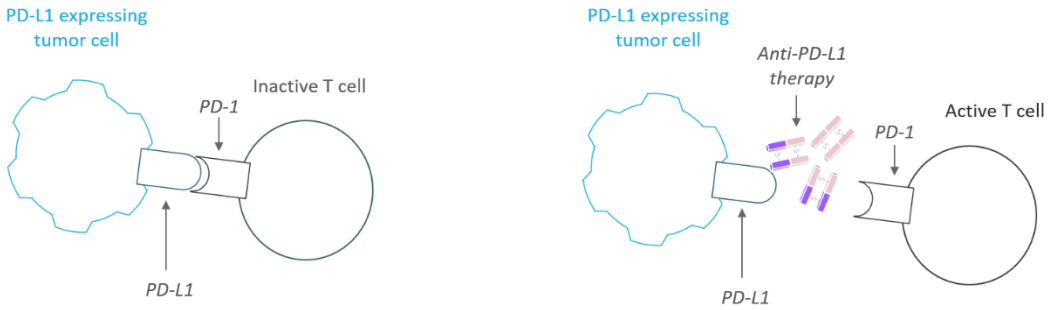

Figure 1.1. — Scheme of immunotherapy for PD-1/PD-L1. Adapted from [18].

1.2 Motivation

Cancer is one of the leading causes of death worldwide, accounting for nearly 10 million deaths in 2020 [2]. Still, cancer survival has almost doubled in the last 40 years [19] because of research efforts in prevention, early diagnosis, and treatment options. The most common cancers are breast, lung, colon and rectum and prostate cancers. Around one-third of deaths from cancer are due to tobacco use, high body mass index, alcohol consumption, low fruit and vegetable intake, and lack of physical activity. The incidence of cancer rises dramatically with age, most likely due to a build-up of risks for specific cancers that increase with age.

Traditional cancer treatments include chemotherapy, radiotherapy, and surgery. However, these are commonly associated with unpleasant side effects such as nausea, fatigue, hair loss, or more severe issues like nephrosis. New research is constantly looking for novel and more refined ways of treating or managing cancer.

Unlike the traditional treatments, immunotherapy is an innovative treatment that dynamically modulates the immune system to attack cancer cells in multiple targets and directions. Immunotherapy is mainly used to strengthen the immune system by regulating the immune microenvironment, so that immune cells can attack tumor cells [20]. In some cases, this alternative therapeutic approach may provide a more efficient treatment, and with fewer side effects; and it can even be combined with other treatments for synergic effect [21].

Programmed death-1 (PD-1) is a cell surface receptor that functions as a T cell checkpoint and plays a central role in regulating T cell exhaustion, which is caused by cancer. Binding of PD-1 to its ligand, programmed death-ligand 1 (PD-L1) that is present in some tumor cells, activates downstream signalling pathways and inhibits T cell activation. Anti-PD-1/PD-L1 therapy has become paramount in cancer therapy, demonstrating increasing beneficial evidence associated with immunotherapy in several cancers (e.g. melanoma, lung, renal cells and lymphoma). Increased evidence on immunotherapy benefits suggests that expression of PD-1/PD-L1 in tissue biopsies is a valuable biomarker for immune checkpoint therapies [22–24].

Nowadays, its expression can only be determined through immunohistochemistry analysis of tissue samples, shown in figure 1.2, requiring invasive methods such as surgical resection or biopsy to obtain tumor material. This can, not rarely, be difficult to perform (due to lesion location and recurrent/metastatic disease). Moreover, checkpoint molecule expression can be very heterogeneous [25, 26].

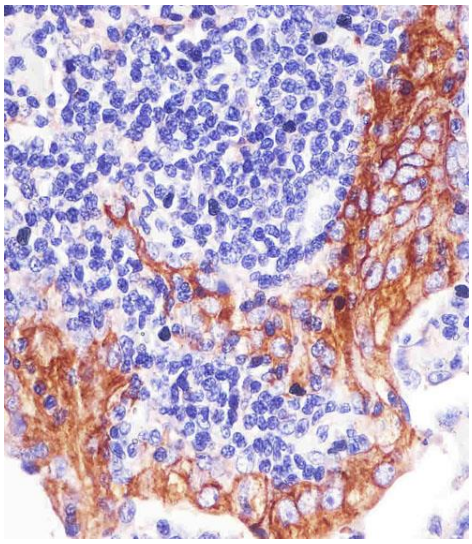

Figure 1.2. — Immunohistochemical analysis of PD-L1. Adapted from [27] .

While PD-1 is expressed by immune system T-cells, PD-L1 is expressed by tumoral cells. Therefore, some research groups have already been focusing their work on PD-L1 and have been developing strategies to label anti-PD-L1 monoclonal antibodies (mAbs) with radionuclides (both single photon emitters and positron emitters). The intention is to image the tumor cellular behaviour rather than imaging the immune system, being Figure 1.3. an example where mice were utilized. Radio-immune-imaging appears to be a promising tool for improving personalized medicine in this field of oncology and immunotherapy [28]. Evidence demonstrates that outcomes are better for patients whose tumors have increasing levels of PD-L1 [29].

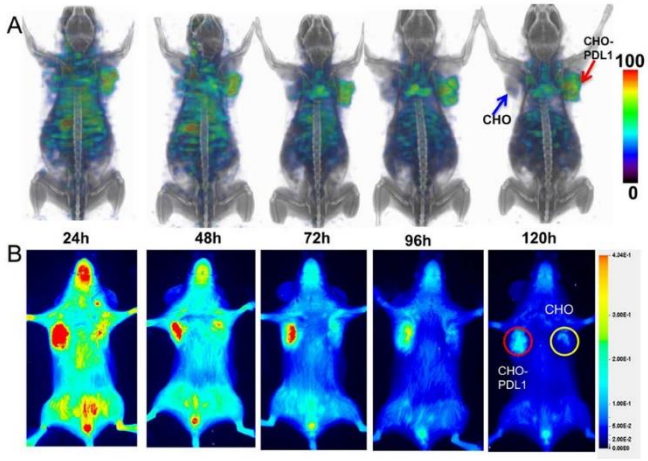

Figure 1.3. — Imaging PD-L1 expression in subcutaneous CHO xenographs. Adapted from [30] .

Atezolizumab (MPDL3280A) was the first monoclonal antibody targeting PD-L1 to be approved for clinical use. Its safety profile and promising efficacy have led to approval for the treatment of advanced NSCLC (Non-small cell lung cancer) and urothelial bladder cancers [31].

Other PD-L1 targeting mAbs can also be of interest for radiolabelling purposes, namely 6E11 (Genentech), a murine mAb which has the advantage of binding not only with PD-L1 positive human cell lines, but also murine cells.

When considering the radioisotope to use for the labelling of mAbs, indium-111 (^{111}In), a gamma emitter, with a half-life of 2.8 days, is especially suited for this purpose since antibodies tend to have long biological half-lives. ^{111}In is a commercially available radionuclide commonly used in clinical routine for SPECT imaging [32].^{111}In forms complexes in which indium is present in the +3-oxidation state, and the open-chain DTPA derivative chelating agents are generally used in ^{111}In nuclear medicine applications. DTPA derivates are capable of coordinating to ^{111}In at room temperature, which can be essential since the antibodies can be degraded at high temperatures [33]. The following Figure 1.4. represents the mentioned coordination.

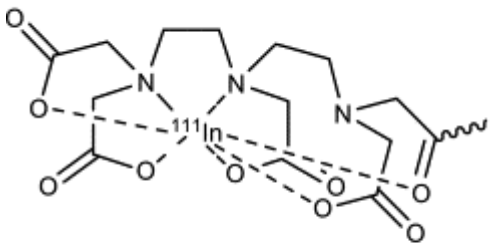

^{111}In-DTPA

Figure 1.4. — Molecular structure of ^{111}In and the chelating agent DTPA (^{111}In-DTPA).

The developed project was intended for diagnosis, once it utilized the radionuclide ^{111}In, which is only used for diagnostic procedures as it doesn't destroy cancer cells.

1.3 Objectives

1.3.1 General aim

This project aims to radiolabel two monoclonal anti-PD-L1 antibodies (Atezolizumab, MPDL3280A; and 6E11) with Indium-111 (^{111}In-DTPA-MPDL3280A; and ^{111}In-DTPA-6E11) to assess *in vitro* the PD-L1 expression in tumor cell lines.

1.3.2 Specific aims

A) To optimize the conjugation of a radiometal chelator to the antibodies;
B) Radiolabel the resulting conjugated antibodies with ^{111}In;
C) Evaluate the cellular binding and uptake of the antibodies in PD-L1-1 positive and negative cell lines.

1.4 Document structure

The present dissertation is composed of 5 chapters, including bibliographic references. The content of each chapter is briefly described bellow:

- Chapter 1. Introduction- Provides context to the studied subject and the main objectives of this work;
- Chapter 2. State of the Art- Presents a review of the literature with the intention of summarizing the past advances on the subject;
- Chapter 3. Materials and Methods- Describes the experimental methodology applied in the various steps of the study;
- Chapter 4. Results' Presentation and Discussion- Reports and discusses the obtained results;
- Chapter 5. Conclusion and Future Work- The main conclusions are summarized as well as this work's future perspectives.

2

STATE OF THE ART

The present research work aims at proposing an approach for addressing viability of monoclonal antibodies as radiopharmaceuticals for cancer immunotherapy. The purpose of this chapter is to briefly introduce the main concepts and previous discoveries that serve as the basis for this thesis.

2.1 Introduction

This state of the art presents existing research and recent updates on the topics of immunotherapy and nuclear medicine in cancer treatment, highlighting the role of the discovered monoclonal antibodies and radionuclides for molecular imaging.

2.2 Immunotherapy in Cancer

Immunotherapy is often perceived as a relatively recent advance. However, one should be looking for the beginnings of cancer immunotherapy under different names as far as in the Antiquity [34].

Known as the father of immunotherapy, William B.Coley, first attempted to harness the immune system for treating cancer in the late 19th century. William B.Coley, in 1909, noted a number of cases in which patients with cancer went into spontaneous remission after developing *Streptococcus* bacteria into tumors, particularly in sarcoma and melanoma patients [35].

Although the idea of unleashing the host immune system to eradicate cancer could trace back to a century ago, [36, 37] significant advances have been achieved in recent investigations. In more recent years, immunotherapy has revolutionized cancer treatment and

rejuvenated the field of tumor immunology, aiming to boost natural defences to eliminate malignant cells. Several types of immunotherapy, including adoptive cell transfer (ACT) and immune checkpoint inhibitors (ICIs), have obtained durable clinical responses, but their efficacies vary, and only subsets of patients can benefit from them [38].

The major categories of cancer immunotherapy include oncolytic virus therapies, cancer vaccines, cytokine therapies, adoptive cell transfer and immune checkpoint inhibitors. A new class of monoclonal antibodies (mAbs) [39], immune checkpoint inhibiters (ICIs) are now entering medical practice and have become one of the most relevant immunotherapies, as shown in Figure 2.1.

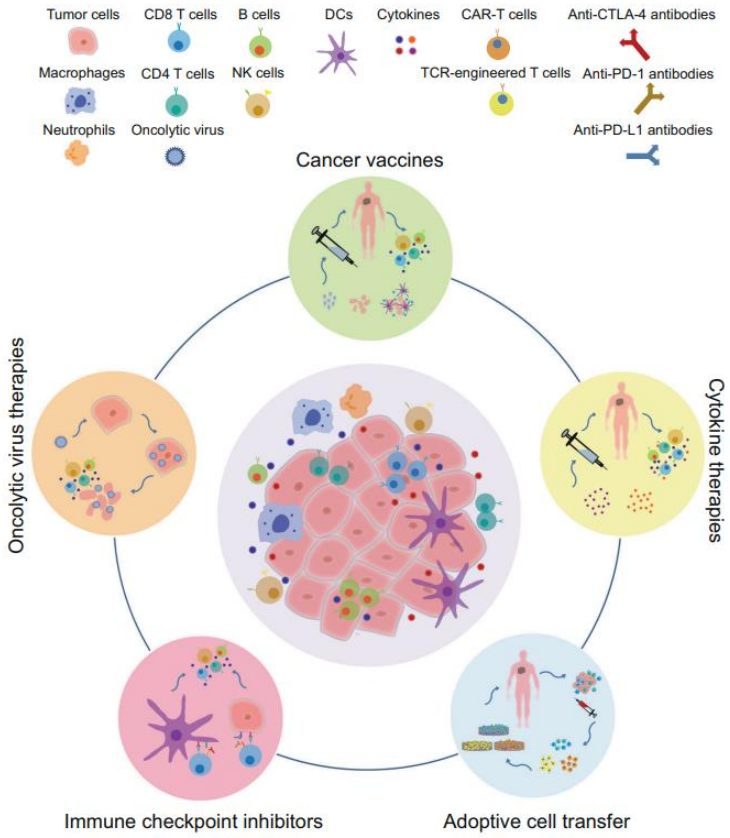

Figure 2.1. — The major categories of immunotherapy, adapted from [38] .

2.2.1 Monoclonal antibodies

Several monoclonal antibodies have been studied and evaluated throughout the years with the purpose of developing anti-cancer drugs. Some of the performed studies found in literature include a variety of antibodies that had been tested and approved by the *Food and Drug Administration* (FDA). Some of those are listed in the Table 2.1.

Table 2.1. — List of mAbs approved for therapy.

Mechanism action	Monoclonal antibody	Clinical indications
HER-2	*Trastuzumab*	Metastatic breast cancer [40, 41]
PD-L1	*Avelumab*	Urothelial carcinoma and Merkel Cell carcinoma [42]
	Atezolizumab	Non-small cell lung cancer, Melanoma, Hodgkin lymphoma, Bladder cancer, Kidney cancer, Breast cancer [43–45]
	Durvalumab	Bladder cancer [42]
PD-1	*Cemiplimab*	Cutaneous squamous-cell carcinoma [42]
	Nivolumab	Melanoma, Lung and Renal cancers [42]
	Pembrolizumab	Melanoma, Various [42]
EGF	*Cetuximab*	Metastatic colorectal carcinoma [46]
VEFG	*Bevacizumab*	Colorectal cancer, Non-small cell lung cancer, Renal cancer, Glioblastoma and Ovarian cancers [42]

The FDA has approved 10 ADCs (antibody-drug conjugates) for cancer treatment and more than 80 ADCs are under clinical investigation (Table 2.2).

Table 2.2. — List of Preclinical mAbs.

Mechanism action	Monoclonal antibody	Clinical indications
G250, CAIX, MN	cG250	Renal cell carcinoma (RCC) [47, 48]
Carbonic anhydrase IX	*Anti-CAIX*	Several cancer types [49]
FAP	*28H1*	Rheumatoid Arthritis [50]
PD-L1	*PD-L1 3.1*	Multiple cancer types [51, 52]
P-cadherin	*FF-21101*	Breast, colon, lung, and pancreas tumors [53]
CEA	*cT84.66*	Colon and rectum, Prostate, Ovary, Lung, Thyroid or Liver tumors [54, 55]
PD-L1	*6E11*	murine Non-small cell lung cancer, pancreatic ductal adenocarcinoma [56, 57]

Amongst the mAbs used in clinical application, Atezolizumab has been of great relevance. It is a high-affinity human IgG1 monoclonal antibody that binds selectively to PD-L1 and prevents the binding of PD-L1 to PD-1, which enhances the magnitude and quality of the tumor-specific T-cell responses, resulting in improved antitumor activity [58, 59].

Tecentriq (Atezolizumab, from *Genetech*), has been approved by the U.S Food Drug Administration (FDA) for various conditions [60] either as a single agent or in combination with other chemotherapeutic agents. Some of it's features are listed in Table 2.3.

Table 2.3. — Tecentriq effectiveness for corresponding tumors.

Clinical indications	Effectiveness
Bladder cancer	- Tecentriq was approved for patients with locally advanced or metastatic urothelial carcinoma regardless of PD-L1 status [61]; - In a clinical study, the ORR was 23.5% of 119 patients [62, 63]; - For patients who had high levels of PD-L1 expression, the ORR was 28.1% and the response lasted a median of 29.7 months [62, 63].
Metastic non-small cell lung cancer (NSCLC)	- FDA approved the medication used in combination with Avastin (Bevacizumab), paclitaxel and carboplatin (chemotherapy) for the initial treatment [64, 65].
Small cell lung cancer	- Tecentriq received approval from FDA to treat patients with extensive small cell lung cancer, in combination with carboplatin and etoposide chemotherapy [66].
Advanced skin cancer (Melanoma)	- Tecentriq was approved to be used in combination with Cotellic and Zelboraf for the treatment of patients with metastic melanoma [67].

Additionally, 6E11, a murine monoclonal antibody clone against PD-L1 that is the *in vitro* equivalent of atezolizumab, has been earning some interest for its application in immunotherapeutic research, with some significant results observed in mouse models (Table 2.4).

Table 2.4. — 6E11 investigation results for the correspondent tumors.

Tumor type	
Pancreatic tumor	High uptake was noted in the spleen and liver (about 3-4 fold higher vs.tumor) as well as blood and lungs [68]
Abdominal tumors	For abdominal tumors such as pancreatic tumors, co-injecting unlabeled antibody at a dose that reduces radiolabeled antibody accumulation in the spleen may facilitate tumor visualization [69]
Non-small cell lung cancer	In the non-small cell lung cancer model, Christensen et al. [70] observed similar uptake of 6E11 in spleen, liver and lungs, with notably lower 6E11 levels in blood

In recent years, several types of immuno-therapies have been developed for cancer treatment, deeply changing paradigms and needs of clinicians, radiologists and nuclear physicians. This new era of personalized medicine for patients with cancer opens new challenges for nuclear medicine and molecular imaging: to deeply understand new clinicians' needs about treatment evaluation imaging and to possibly propose new imaging and therapeutic tools by radiolabelling monoclonal antibodies [71].

2.3 Nuclear Medicine

The origins of nuclear medicine go back to 1895, the year x-rays and the concept of ionizing radiation were discovered. X-rays were reported by Roentgen, a German physics professor, when he was studying light emissions generated by electrical discharges. Only a year after, 1896, x-rays were utilized in medicine. Radioactivity was only discovered by Becquerel in 1896, who demonstrated that radiation emitted by uranium was similar to x-rays but, unlike x-rays it could be disturbed by a magnetic field, concluding then that it consisted of charged particles [72].

Marie Curie, who worked with her husband, inspired by Becquerel, revolutionized the concept of radioactivity by showing that the intensity was independent of the form of uranium, and rather was proportional to the amount, confirming that it was a property of the element itself. The unit of radioactivity, Curie (Ci) was named after Marie Curie [72]. A consummate experimentalist, Rutherford (1871-1937) discovered *alpha* and *beta* rays, proposed the laws of radioactive decay, and postulated the nuclear structure of the atom [73].

Nuclear Medicine is a medical specialty that evaluates physiology and tissue metabolism *in vivo* with tracer techniques. The tracers used for these studies are generally short-lived radionuclides and are linked to chemical compounds that permit specific physiologic processes to be imaged/or quantified non-invasively. The role of nuclear medicine has changed dramatically in the last decade, due to advances in radiopharmaceuticals and imaging technology. Radiopharmaceuticals are a class of pharmaceutical drugs containing radioactive isotopes. Radiopharmaceuticals can be used as diagnostic and therapeutic agents.

Evolving areas of clinical utility include the increased role of nuclear medicine in therapy; the introduction of Positron Emission Tomography (PET); and the development of new radiolabelled molecules for the biological characterization of human tissues, which has both clinical and research applications [74]. A wide range of radionuclides with different characteristics have been used to radiolabel molecules, some are characterized in Table 2.5.

Table 2.5.— Examples of radionuclides used in nuclear medicine.

Radionuclide	Half-life	Energy (KeV)	Emitter	Source
^{64}Cu	12.7 h	653	β+	Cyclotron
^{67}Ga	78.3 h	93.185	ɣ	Cyclotron
^{89}Sr	50.6 h	1460	β-	Reactor
^{90}Y	64.1 h	2270	β-	Reactor
^{99m}Tc	6.02 h	141	ɣ	Generator
^{111}In	67.9 h	171.247	ɣ	Cyclotron
^{153}Sm	46.3 h	702.810; 103	β-, ɣ	Reactor
^{177}Lu	6.7 d	176,497;113,208	β-, ɣ	Reactor
^{186}Re	90.6 h	936.1070;137	β-, ɣ	Reactor
^{201}Tl	73.1 h	135.167	ɣ	Cyclotron
^{131}I	8 d	971	β-, ɣ	Reactor
^{89}Zr	78.4 h	396	β+	Cyclotron

2.3.1 Molecular Imaging

Molecular imaging includes the field of nuclear medicine, which uses very small amounts of radioactive materials (radiopharmaceuticals) to diagnose and treat disease. In nuclear medicine imaging, the radiopharmaceuticals are detected by cameras that work with computers to provide accurate imaging of living organisms [75]. Molecular imaging has two basic applications. The first is diagnostic imaging, which is used to determine the location and extent of targeted molecules specific to the disease being assessed. The second is therapy, which is used to treat specific disease-targeted molecules [76].

Molecular imaging techniques depend upon molecular mechanisms operative *in vivo*. The techniques used include Positron Emission Tomography-Computed Tomography (PET-CT), Magnetic Resonance Imaging (MRI), and Single Photon Emission Computed Tomography (SPECT). The most used techniques in nuclear imaging are SPECT and PET, schemed in the Figure 2.2.

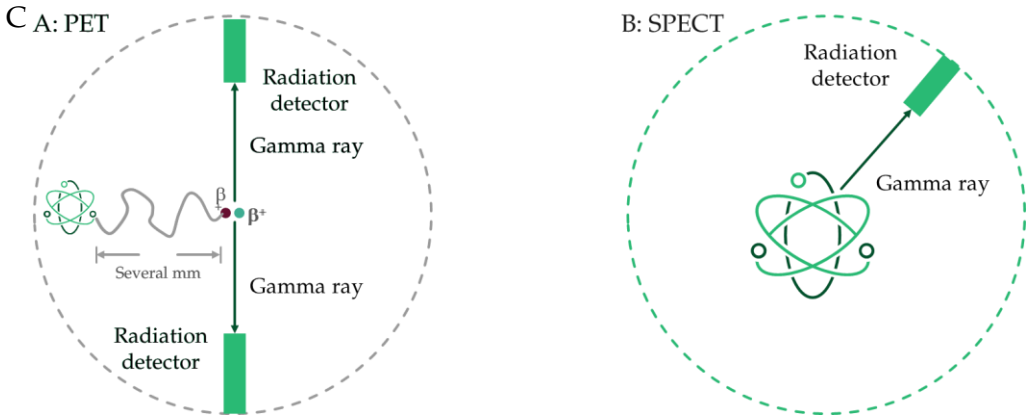

Figure 2.2. — Illustration of PET and SPECT. Adapted from [77].

SPECT imaging instruments provide three-dimensional (tomographic) images of the distribution of radioactive tracer molecules that have been introduced into the patient's body. The 3D images are computer generated from many projection images of the body recorded at different angles. SPECT imagers have gamma camera detectors that can detect the *gamma ray* emissions from the tracers that have been injected into the patient. The cameras are mounted on a rotating gantry that allows the detectors to be moved in a tight circle around a patient who is lying on a pallet [78] as well as planar images.

PET is a rapidly developing nuclear imaging technique, with a clinical role that now exceeds almost 15 years [79]. PET scans also use radiopharmaceuticals to create three-dimensional images. The main difference between SPECT and PET scans is the type of radiotracers used. While SPECT scans measure *gamma rays*, the decay of the radiotracers used with PET scans produce small molecules called *positrons*. A positron is a particle with roughly the same mass as an electron but oppositely charged. These react with electrons in the body and when these two particles combine, they annihilate each other. This annihilation produces a small amount of energy in the form of two photons that shoot off in opposite directions, and with equivalent energy (511 keV). The detectors in the PET scanner measure these photons and use this information to create images of internal organs. [78]

Theoretically, almost any radionuclide can be chemically attached to a molecule, but the choice will depend upon the application. Although justification of a particular choice is usually not included in published reports, implicit are those factors extensively discussed decades ago [80]–[82], including (1) decay type, (2) physical half-life, (3) availability and (4)

ease of labeling. In general, radionuclides with short physical half-lives are preferred for imaging to minimize the radiation exposure. However, a too short half-life may not provide sufficient time for radiolabeling. Furthermore, the half-life must be a good match to the time between administration and imaging that is required to reach an adequate target/nontarget ratio that can vary over a wide range depending upon the application.
The half-lives of many of the metallic radionuclides, including zirconium-89 [83] (78 h half-life) for PET, and indium-111 [84] (67 h half-life) for SPECT, more closely match the time required for antibodies to clear circulation and accumulate in target tissue than non-metallic radionuclides such as fluorine-18 (119 min half-life).

^{111}In is a commercially available radionuclide commonly used in clinical routine for SPECT imaging, that decays 100% by electron capture leading to emission of two low energy *gammas* (171, 245 keV), making indium-111 a suitable radionuclide for SPECT imaging. Because a strong and stable bond does not form directly between radiometals and mAbs, researchers use bifunctional chelating agents. DTPA and DOTA are the frontrunners for indium chelation, because of their availability and stable coordination of the ^{111}In ion. Both perfectly coordinate indium with its preferred coordination number of 8. DTPA and DTPA derivatives, including CHX-A″-DTPA, form very stable square antiprism-like structures with ^{111}In using N_3O_5 bonds, and have been utilized in several radiopharmaceuticals approved for clinical use [94].

Radiolabeling of antibodies with In-111 has now been accomplished to the point that it is highly reproducible, achieves excellent labeling efficiency, and does not damage the antibody. The use of ^{111}In for radio immunodetection is advantageous because of the excellent imaging characteristics of the ^{111}In, moderate radiation dose, ease of labeling, and appropriate half-life. The liabilities of the ^{111}In method include slightly greater cost of the radionuclide, slow clearance of background sites, and a shelf life requiring it to be ordered on a weekly basis [86].

Table 2.6. highlights the differences between PET and SPECT imaging.

Table 2.6. — Strength and weakness of the main available imaging modalities used in molecular imaging, adapted from [87] .

Imaging Modality	Electro magnetic radiation spectrum	Advantages	Disadvantages
Positron Emission Tomography (PET)	High energy gamma rays	High sensitivity, shorter time scan, enable quantitative analysis	PET cyclotron or generator needed, relatively low spatial resolution
Single Photon Emission Computed Tomography (SPECT)	Lower energy gamma rays	Many molecular probes available, can image multiple probes simultaneously, may be adapted to clinical imaging system	Relatively low spatial resolution, high radiation to subjects due to longer tracer half-lives, non-quantative tool, longer scanning time

2.3.1.1 Radiolabelling

The use of radionuclide labels allows the study of the pharmacokinetics of monoclonal antibodies, to control the specificity of their targeting and to monitor the response to an antibody treatment with high accuracy. Since radiolabelling procedure might damage and reduce the immunoreactive fraction and/or affinity to an antibody, the methods for the radiolabelling must be the suitable ones minding the utilized antibody [88].

While radiolabelling is preferably fast, mild, efficient, and reproducible, especially when applied for human use in a current Good Manufacturing Practice compliant way, it is crucial that the obtained radioimmunoconjugate is stable and shows preserved immunoreactivity and *in vivo* behaviour. Radiometals and chelators have extensively been evaluated to come to the most ideal radiometal–chelator pair for each type of antibody derivative [89].

2.3.1.1.1 Chelation

Chelation is a type of bonding of ions and molecules to metal ions. It involves the formation or presence of two or more separate coordinated bonds between a polydentate (multiple bonded) ligand and a single central metal ion [90].

Advances in nuclear imaging adequate methods for labelling compounds with a variety of radionuclides [91]. Radionuclides have been used to label bioactive molecules including oligomers, often by isotope substitution. While labelling by isotope substitution essential-

ly guarantees that the properties of the biological will not be altered, the labelling process is usually nontrivial. With few exceptions, biologicals cannot be radiolabelled with metallic radionuclides in this matter but require the preliminary covalent attachment of a chelator, a chemical structure capable of binding a metal [92]. The conjugation of chelators to antibodies is executed to permit the coordination between the antibody and the radionuclide, since the chelating agent will bind to radiometal ions [93].

Various types of chelators have been studied to this date; amongst them, MAG3, DOTA and DTPA derivatives, have been some of the most explored in radiopharmaceutical development. When labeled with ^{99m}Tc, mercaptoacetyltriglycine (MAG_3) is a clinical radiopharmaceutical for imaging kidney function [95]. Because of its ability to stabilize chelate ^{99m}Tc, MAG_3 has also been modified into a bifunctional chelator for the labeling of biologicals. A NHS (N-Hydroxyl succinimide) activated MAG3 bifunctional chelator (Figure 2.3) (S-acetyl NHS-MAG3) has been used for the labeling of amine derivatized oligomers with ^{99m}Tc. To avoid the harsh conditions of boiled water temperature and alkaline pH of benzoyl deprotection, S-acetyl NHS-MAG3 was synthesized in which an acetyl replaces the benzoyl group. As a better leaving group, acetyl can be more easily removed at neutral pH and room temperature [96]. Like most chelators useful with ^{99m}Tc, MAG3 can also form stable complex with ^{186}Re and ^{188}Re, because of similarities in the chemistry of technetium and rhenium.

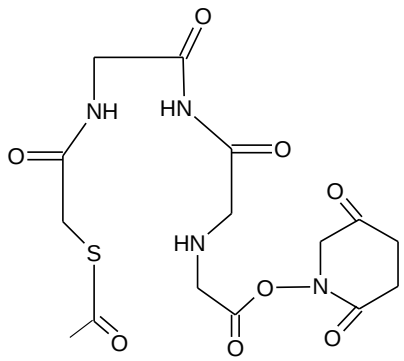

Figure 2.3. — Structure of the conjugated NHS-MAG_3.

1,4,7,10-Tetraazacyclododecane-N,N‘‘,N‘‘‘‘,N‘‘‘‘‘‘-tetraacetic acid (DOTA) is a good chelator for trivalent metals, such as In3+ , Y 3+ and other metals of the lanthanide series [97] and can be readily modified into a bifunctional chelator, although by first activating a carboxylate with a carbodiimide as with DTPA, DOTA itself may be conjugated. Alternatively, DOTA bifunctional chelators may be prepared by derivatization of one of the carboxylates, and their NHS or SCN activated derivatives. The DOTA chelator structure is shown in Figure 2.4.:

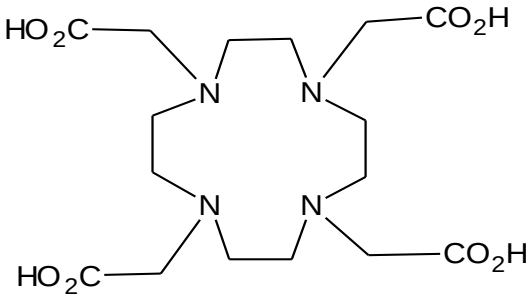

Figure 2.4. — DOTA chelator.

DOTA is a macrocycle with a 12-membered tetraazide macrocycle ring and due to its rigid structure, its radiometal complexes tend to be kinetically inert to dissociation and are also characterized by high thermodynamic stability [98, 99].

Although the active DTPA ester formed in situ by reacting with a carbodiimide such as EDC [1-Ethyl-3(3-dimethylaminopropyl) carbodiimide Hydrochloride)] has been used for the conjugation of DTPA to biologicals [100], DTPA in the form of a bifunctional chelator has proved to be more used. As the simplest bifunctional form of DTPA, the cyclic DTPA anhydride has been widely used[101]. However, unlike ^{99m}Tc-MAG3, the ^{99m}Tc within the DTPA chelator is susceptible to oxidation once the excess Sn (II) used in the labeling is removed. Furthermore, the labeling efficiency is usually low because DTPA is a poor chelator for ^{99m}Tc [102].

As such, DTPA, schematized in Figure 2.5, has seen more use for attaching trivalent metals such as ^{111}In, [103] or even lanthanides such as ^{90}Y [104]. The labeling kinetics of DTPA for ^{111}In is typically fast, and an almost quantitative labeling efficiency is usually achieved even at neutral pH and room temperature. This method of labeling is therefore suitable for biologicals sensitive to excessive heat and acidity.

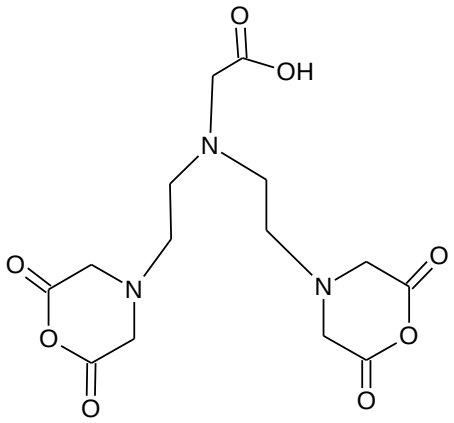

Figure 2.5. — Structure of cyclic DTPA.

Earlier there was a concern that the use of the cyclic DTPA anhydride could cross link two biologicals because of the two anhydride groups [105]. However, no direct evidence of cross linking has been reported. A plausible explanation is that the cyclic DTPA anhydride is normally added at a five-fold molar excess or higher. The excess anhydride is also often necessary to compensate for the hydrolysis of the anhydride that will occur in aqueous solution in competition with conjugation. Another concern to the use of the cyclic anhydride is the possible compromised chelation stability because of the loss of one carboxylate to the conjugation [106]. The following Figure 2.6 represents the DTPA derivative used in the project.

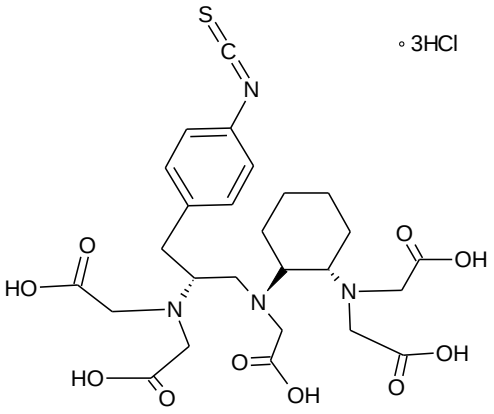

Figure 2.6. — Scheme of p-SCN-Bn-CHX-A”-DTPA molecular structure, adapted from [107].

3

MATERIALS AND METHODS

All commercially acquired chemical reagents and solvents were of pro-analysis quality and were used without any additional purification. MPDL3280A was from *Tecentriq*, 6E11 from *Genentech*, p-SCN-Bn-CHX-A"-DTPA from *Macrocyclics* and [^{111}In]$InCl_3$ from *Mallinckrodt.*

3.1 MPDL3280A and 6E11 purification and conjugation with a DTPA derivate

3.1.1 Excipient removal for MPDL3280A and 6E11

10 mg of MPDL3280A (144 612.59 g/mol) was diluted with H_2O to 4 mL. The solution was inserted in an *Amicon ultra® Centrifugal Filter* (*Merck* [108]) (previously washed with NaCl 0.9%); and the filter went through centrifugation at 3 000 rpm for 30 minutes. After that, the solution went through a second wash with H_2O, under the same conditions.
The purification of 6E11 was performed in parallel, and the procedure followed the exact same steps.

3.1.2 Conjugation of DTPA to MPDL3280A and 6E11

The antibodies obtained from 3.1.1 were placed in a 5 mL *eppendorf* tube and diluted in a sodium bicarbonate buffer (0.1 M and pH=9.5) to 2,5 mL. 330 µL of p-SCN-Bn-CHX-A"-

DTPA (0.01 M, H_2O) were added (in a molar ratio of 1:50 mAb:chelator). The solutions were then left to stir for one hour at room temperature.

To remove the unbounded DTPA, the solutions were centrifuged in an *Amicon ultra®* filter (previously washed with NaCl 0.9%) at 3 000 rpm for 30 minutes. After that, the solutions were washed twice with Ammonium Acetate (0.1 M, pH 5.5) and twice with H_2O.

3.1.3 Characterization of the conjugates

3.1.3.1 QTOF analysis

The conjugated antibodies were characterized through the technique *Intact mass determination by X500B QTOF with Twin-spray ion source* was performed by the ITQB/iBET lab, supported by Professor Mário Eusébio's group from FCT-NOVA.

The sample was subjected to an ultrafiltration clean-up procedure using 10 kDa cutoff filtration units with water/0.1% FA (LC-MS grade). The data was acquired in positive TOF-MS (Time of Flight Mass Spectrometer) mode using a X500B QTOF with Turbo V ion source (Sciex) mass spectrometer connected to the ExionLC AC UPLC system.

3.1.3.2 Determination of concentration using *Nanodrop*

Preparation of the sample solutions was performed by initially using 33.2 µL of the MPDL3280A solution (1200mg/mL) diluted with H_2O to 500 µL. From this first solution (4 mg/mL), 5 more were obtained through dilution in order to obtain concentrations as depicted in Table 3.1.

Table 3.1.— Concentrations of the MPDL3280A solutions.

Solution	Concentration (mg/mL)
1	4
2	2
3	1
4	0.5
5	0.25
6	0.125

The resulting solutions were then analysed by Nanodrop. The *Nanodrop 2000* spectrophotometer from *Thermo Fisher Scientific* [109] is a full-spectrum, UV-Vis spectropho-

tometer used to quantify and assess purity of DNA, RNA, protein and more. With the results from Nanodrop, a calibration curve, presented in the following chapter, was obtained.

3.2 Radiolabelling of MPDL3280A-DTPA and 6E11-DTPA

3.2.1 Radiolabelling of the conjugates

3.2.1.1 Radiolabelling procedure

The radiolabelling procedure was based on a protocol found in the literature [110].

In a 1.5 mL *eppendorf* tube containing 0.25 µL of Sodium Chloride (NaCl) 0.2 M and 0.03 µL Ammonium Acetate (NH_4OAc) 3 M, at pH=7, 0.2 mg of the DTPA-containing mAb was added. 16 µL of ^{111}In (2.8 days of semi-life) in the form of Indium Chloride $[^{111}In]InCl_3$ was added to the solution. It was confirmed that the pH value was 7 by the means of a pH tape. The mixture was kept at room temperature for 1 h.

3.2.1.2 Radiochemical yield

The control of the radiochemical yield was performed by iTLC, with a stationary phase of silica-gel chromatography layer and sodium acetate (0.1 M, pH=5) as eluent [110].

The yield was calculated through the ratio between the measured radioactivity at the sample application point of the layer and the total measured radioactivity, presented in equation (1):

$$\text{Radiolabelling yield} = \frac{\text{Radioactivity at the application point}}{\text{Radioactivity at the application point+Radioactivity at the solvent front}} \times 100 \qquad (1)$$

3.2.1.3 Purification of the radiolabelled conjugates

After the radiolabelling, the conjugates went through a purification step with the purpose of removing the unbounded [^{111}In]InCl$_3$ by ultrafiltration with an *Amicon Ultra 10 K centrifugal filter device*, using PBS 0.1 M. The mixtures were centrifuged for 30 minutes and 3 000 rpm.

3.2.1.4 *In vitro* stability studies

Different *eppendorfs* containing 20 µL of radiolabelled mAb solution were added 40 µL of cell culture medium RPMI, DMEM, and NaCl 0.9%.
The mixtures were incubated at 37ºC and analysed by iTLC at different time points: 1 h, 24 h and 48 h.

3.3 Biological Evaluation Studies

3.3.1 Cell lines

Two human cell lines of non-small cell lung (H2444) and triple negative breast cancers (MCF-7); and five murine cell lines of Lewis lung cancer (LLC), melanoma (B16F10), triple negative breast cancer (E0771) and multiple myeloma (MM) (MOPC315 and MOPC315.BM) were used.

H2444, MCF-7, E0771, LCC and B16F10 cell lines were thawed and maintained in RPMI; and MOPC315 and MOPC315.BM in DMEM, both media supplemented with 10% Fetal Bovine Serum and 1% of penicillin/streptomycin at 37 ºC and 5% CO_2. Cells were split every two or three days.

.

3.3.2 Flow Cytometry

To assess PD-L1 expression, the seven cell lines (human and murine) were collected and plated. Cells were centrifuged and incubated with an FC-block (perform the saturation of the Fc antibody receptors to block unspecific binding) anti-human and anti-mouse, respectively for 10 min at 4 ºC. After blocking, the cells were washed with PBS and then the viability dye

Invitrogen (Thermo Fisher Scientific) was added to exclude dead cells from the analysis. After a third washing, the antibodies, were added separately to the cell lines and incubated for twenty minutes at 4º C- MPDL3280A and MPDL3280A-DTPA were added to the human cell lines, and 6E11 and 6E11-DTPA to the murine ones. Control studies were performed in parallel using protein PD-L1 BV711 which was added to all cell lines. Cells were washed and 1:100 IgG anti-human APC (Allophycocyanin) and 1:200 IgG anti-mouse PE were added to the human and murine cell lines, respectively.

After washing the samples, cells were filtered and analyzed on a FAS Fortessa x20 (BD Biosience). Compensation was used using beads. Data was analyzed using the FlowJo software.

3.3.3 Cellular uptake assays

Cellular uptake studies were performed based on a protocol found in literature [111].

Initially, the cells were plated in quadruplicate in 24-wells cell culture plates at a concentration of $2.5x10^5$ cells/well for MCF7 and LLC cells lines, $1.25x10^5$ cells/well for H2444 cell line, and $0.6x10^5$ cells/well for MOPC315 cell line, in 500 µL of complete culture media, and incubated at 37 ºC and 5% CO_2.

The following day, the cell culture medium was removed, and the adherent cells incubated with approximately 20 KBq of ^{111}In labelled antibodies in 500 µL (humified atmosphere with 5% CO_2 at 37ºC). At each of the 5 time points (1h, 2h, 4h, 20h, 24h), the supernatant was removed and the cells were washed twice with cold PBS. The cells were then lysed with 1 M NaOH and the lysates transferred to tubes and measured with a ATOMLAB Wipe Teste Counter (Biodex) to assess cell associated activity.

4

RESULTS' PRESENTATION AND DISCUSSION

The *Champalimaud's Foundation* Radiopharmacology Research Group has been studying and developing new radioligands (radiopharmaceuticals as biomarkers) from the bench to the clinical applications, following the radiopharmaceutical and radioprotection regulations to search for continuing improvement of diagnosis and therapy in oncology [112].

4.1 Synthesis and characterization of DTPA-containing mAbs

The first step of the experiment consisted in conjugating the antibodies Atezolizumab and 6E11 with a diethylenetriaminepentaacetic acid (DTPA) derivate (p-SCN-Bn-CHX-A"-DTPA). This would allow the radiometal ^{111}In to bind to the antibody through chelation with the DTPA.

Before conjugation, an ultracentrifugation process was performed for MPDL3280A and 6E11 using an *Amicon ultra® Centrifugal Filter* (*Merck* [108]) and washed with H_2O, with the purpose of removing the excipients that might be present in the sample and that could interfere with the conjugation of the chelator.

The resulting mAbs were then reacted with an excess of a DTPA derivate (50:1), p-SCN-Bn-CHX-A"-DTPA, in sodium bicarbonate buffer (pH=9.5) and at room temperature for 1 h. The thyocianate group of p-SCN-Bn-CHX-A"-DTPA allows the formation of thiourea bonds with free amine groups within the mAbs [113], [114].

The unbounded DTPA was removed by ultrafiltration and washed with PBS 0.1 M.

Figure 4.1 schematizes the reaction of conjugation of the mAbs to the chelator.

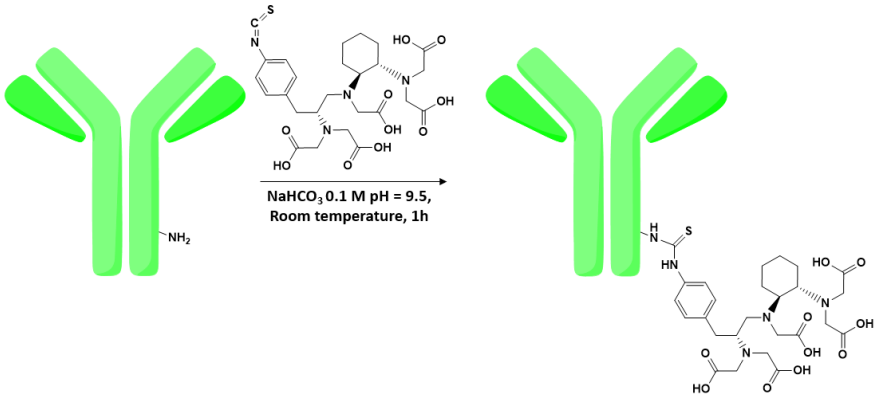

Figure 4.1. — Scheme of the reaction of conjugation of the mAb to DTPA.

In order to assess the conjugation of the DTPA derivative to the mAbs, a Q-TOF-MS analysis was performed for both conjugates.

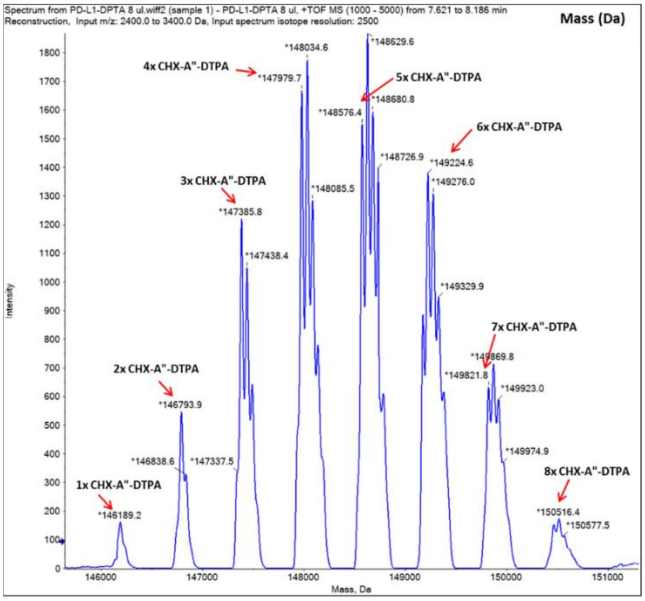

Figure 4.2. — Mass spectrum presenting the range of DTPA molecules attached to MPDL3280A.

The mass spectrum showed in Figure 4.2. confirms the conjugation of the DTPA derivative to MPDL3280A. Various species were observed in the spectrum with a constant mass difference of 590-595 Da. This is consistent with the addition of p-SCN-Bn-CHX-A"-DTPA molecules (595 Da) to the antibody (145661 Da). Thus, the number of conjugated DTPA molecules per mAbs varies, ranging between 1 to 8, which is to be expected due the various binding sites available in the antibody structure [115].

Similarly, for 6E11, the conjugation of DTPA was also successful. However, a higher amount of conjugated DTPA was observed as seen in Figure 4.3, ranging from 5 to 9 chelator molecules per mAb.

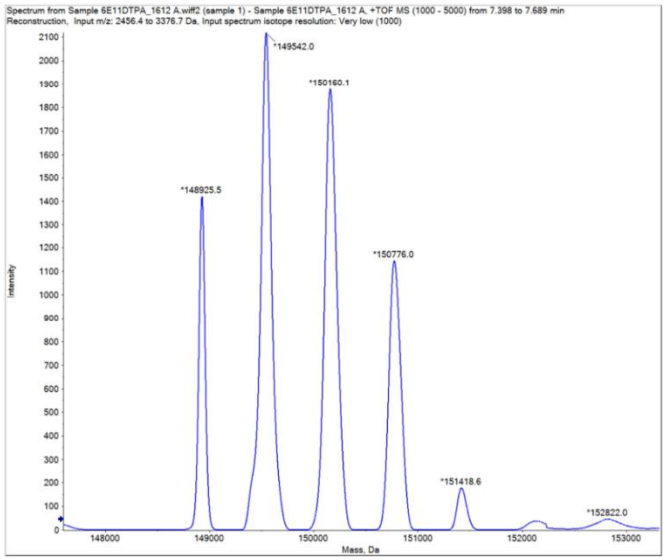

Figure 4.3. — Mass spectrum presenting the range of DTPA molecules attached to 6E11.

4.1.1 Concentration of the conjugates

In order to determine the concentration of the DTPA-containing mAbs solutions a *Nanodrop* equipment was used. A calibration curve was initially obtained using sample solutions of MPDL3280A (Figure 4.4), with the purpose of finding if the spectrophotometer was reliable for concentration measures.

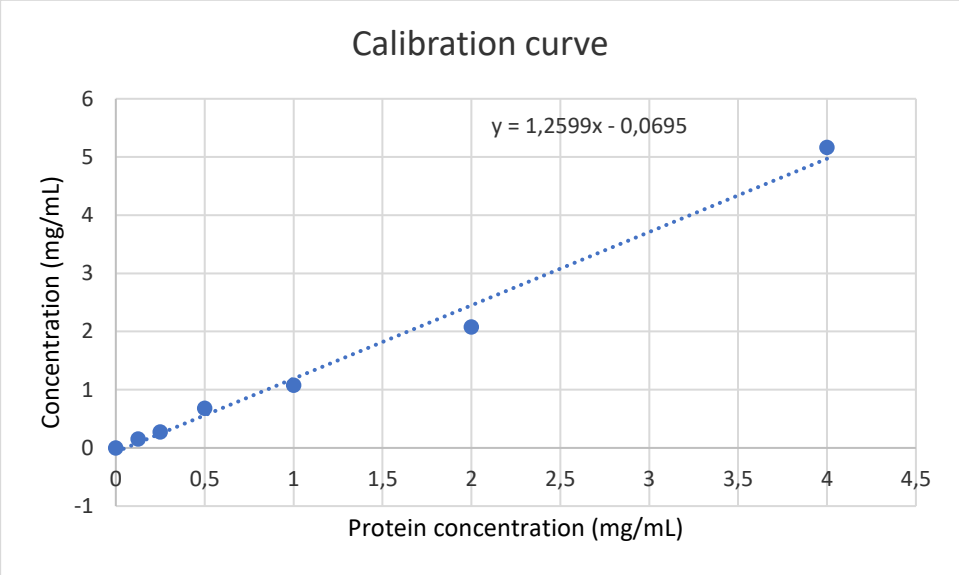

Figure 4.4. — Calibration curve for the samples the correspondent concentrations.

When measuring the sample of MPDL3280A-DTPA a value of 2.239 mg/mL was obtained from the spectrophotometer. When applied in the equation of the calibration curve (equation (2)), the result was 1.83 mg/mL:

$$y = 1.2599x - 0.0695 \tag{2}$$
$$y = 1.2599 \times 2.239 - 0.0695 \leftrightarrow y = 1.83$$

From the equation, we obtained the exact value of the sample.

The degree of variation between the measured value and the value calculated through the calibration curve is not significant, which indicates that the spectrophotometer could provide feasible results, and could be used for further direct measurements.

4.2 MPDL3280A-DTPA and 6E11-DTPA labelling with ^{111}In

4.2.1 Radiolabelling procedure

The radiolabelling of the of the DTPA-containing mAbs was performed based on a procedure found in literature [110]. Briefly, the mAbs were reacted with $^{111}InCl_3$ in a mixture of NaCl 0.9% and sodium ammonium acetate at pH = 7, at room temperature for 1 h, represented in Figure 4.5.

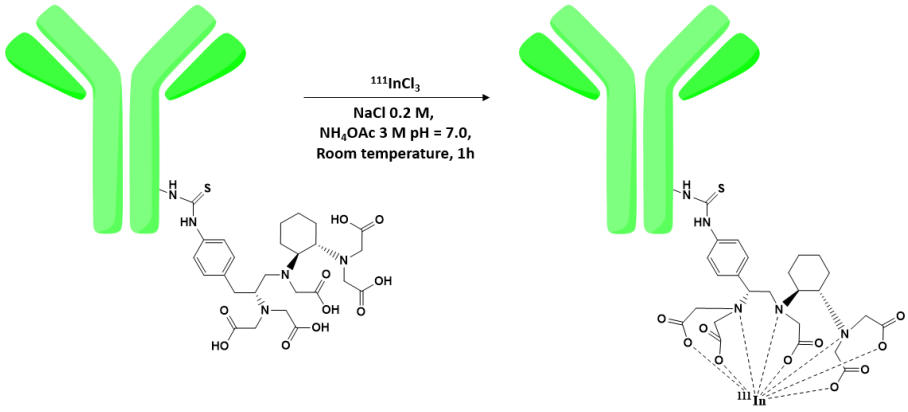

Figure 4.5. — Scheme of the reaction of radiolabelling of the mAb-DTPA with ^{111}In.

The control of the radiolabelling yield was done by iTLC [110], with results of approximately 75% and 60% for MPDL3280A-DTPA and 6E11-DTPA, respectively. In parallel, a similar radiolabelling procedure was also performed using MPDL3280A without conjugated DTPA. iTLC analysis showed no significant labelling of the mAbs with ^{111}In, which indicates that the radiometal is bound to the mAbs through DTPA chelation.

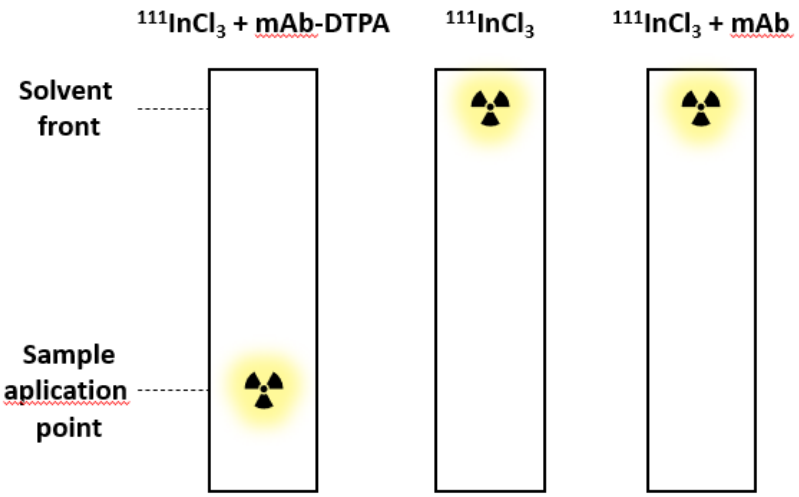

Figure 4.6. — Scheme of TLC layers of $^{111}InCl_3$ labelled mAb-DTPA, free $^{111}InCl_3$ and $^{111}InCl_3$ labelled mAb.

In order to optimize the radiolabelling yield slight modification to the procedure were performed, using MPDL3280A-DTPA. These included variation of temperature, pH and ligand concentration (Table 4.1).

Table 4.1.— Radiolabelling yield of the conjugate MPDL3280A-DTPA with the variations 1-3.

Variation	Temperature (°C)	pH	mAb quantity (mg)	Yield (%)
1	40	7	0.2	75
2	room	7	0.4	80
3	room	6	0.2	75

The results shown on Table 4.1 indicate that no significant improvement of the radiochemical yield was observed. Hence, it was required to purify the radiolabelled mixture in order to remove the unreacted ^{111}In.

4.2.2 Purification of the radiolabelled conjugates

Purification of the radioconjugates was performed by ultrafiltration with the use of an *Amicon Ultra 10 K centrifugal filter device* and washed with PBS 0.1M.

After the purification, iTLC was done to evaluate the radiochemical purity of the labelled mAbs. Results obtained showed a > 95% purity degree for both ^{111}In-MPDL3280A and ^{111}In-6E11-DTPA.

4.2.3 *In vitro* stability studies for ^{111}In-MPDL3280A-DTPA and ^{111}In-6E11-DTPA

In vitro stability studies were performed to assess if the radiolabelled complexes were stable in different challenging media, including 0.9% NaCl and cell culture media RPMI and DMEM.

The sample mixtures were incubated at 37ºC, and an iTLC was performed for each sample at specific time points: 1 h, 24 h, and 48 h (Figures 4.7 and 4.8):

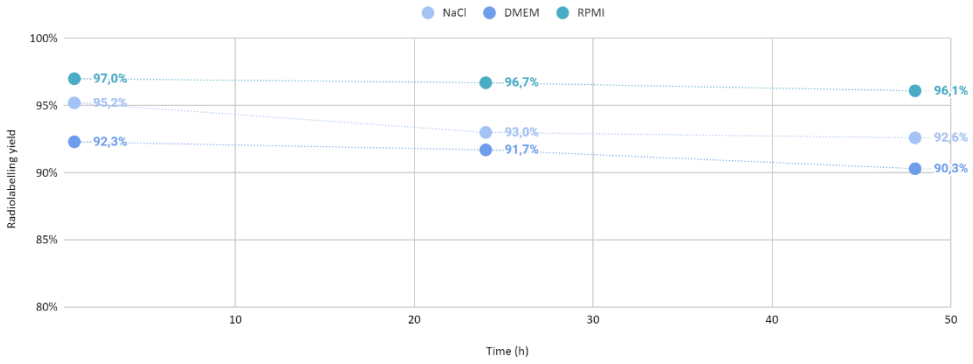

Figure 4.7. — MPDL3280A-DTPA radiolabelling yield after 1h, 24h and 48h in the three mediums.

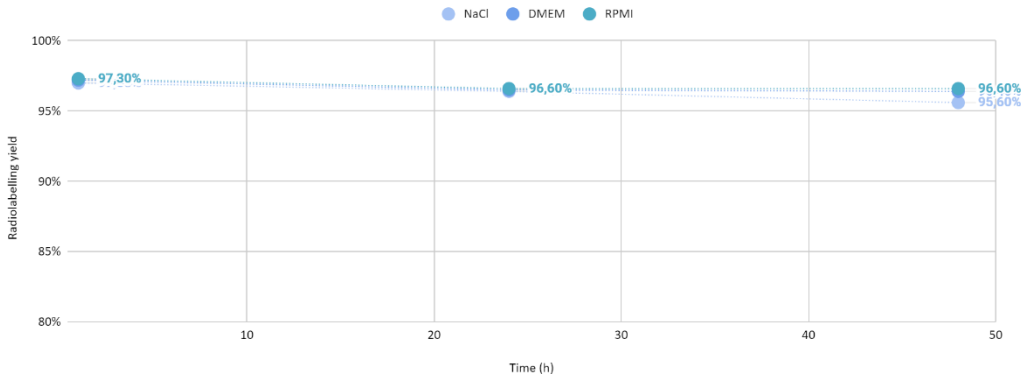

Figure 4.8. — 6E11-DTPA radiolabelling yield after 1h, 24h and 48h in the three mediums.

Results showed a suitable radiochemical stability of both ^{111}In-labelled mAbs in the different media, with values of >90% of radiolabelled compound after 48 h of incubation.

4.3 Biological Evaluation Studies

4.3.1 Flow Cytometry

Flow cytometry was utilized with the purpose of assessing the expression of the surface protein PD-L1, and to evaluate the binding capability of the mAbs to it. BV711 was used as control mAb, since it is known to bind effectively with PD-L1.

The studies were performed in high PD-L1 expressing human and murine cell lines: H2444 (human lung cancer cells) and MOPC315 (murine melanoma cells); and in low expressing PD-L1 cell lines: MCF7 (human breast cancer cells), E00771 Luc+ (murine breast cancer cells), LLC (murine lung cancer cells), B16F10 (murine melanoma cells) and MOPC315 BM (murine melanoma cells). MPDL3280A and MPDL3280A-DTPA were evaluated in the human cell lines, while 6E11 and 6E11-DTPA were evaluated in the murine ones. Results are reported in Figures 4.9 and 4.10.

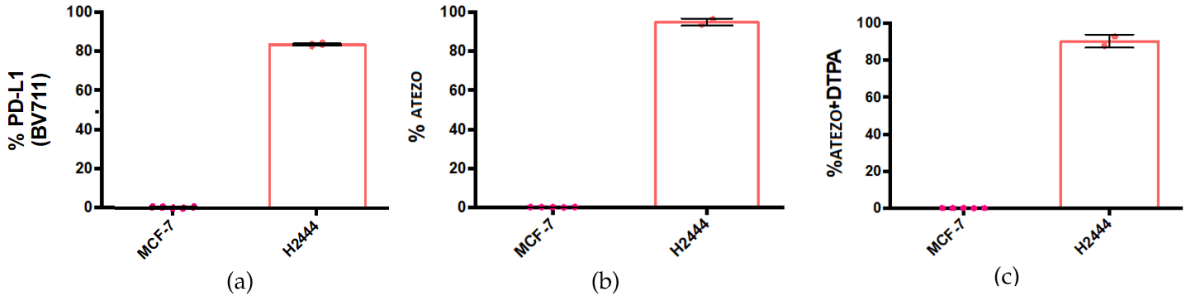

Figure 4.9. — PD-L1 expression in human cell lines binded to: a) Protein BV711 (control), b) MPDL3280A, c) MPDL3280A-DTPA.

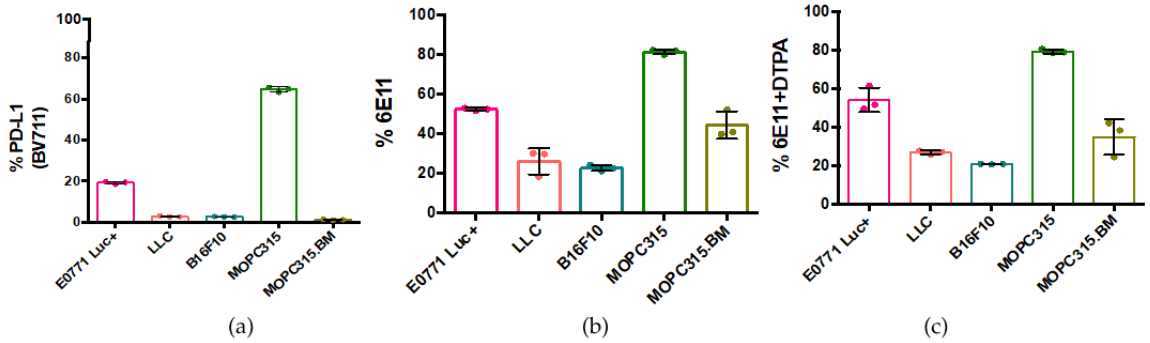

Figure 4.10. — PD-L1 expression in murine cell lines binded to: a) Protein BV711 (control), b) mAb 6E11, c) 6E11-DTPA.

The control results with BV711 for the human cell lines, show a high expression of PD-L1 for H2444 (95.3%) cell lines, while for MCF7 the expression was negligible (0.04%). When incubated with MPDL3280A and MPDL3280A-DTPA, the expression of PD-L1 was comparable to that of the control BV711, with values of 95.1% and 90.3%, respectively.

In the case of the murine cell lines, MOPC315 showed the highest PD-L1 expression when incubated with BV711 (64.6%). E0771 Luc+ displayed a low expression of PD-L1 (19.2%), while for LLC, B16F10 and MOPC315 BM, the values were negligible (<5%). Interestingly, when incubated with 6E11 or 6E11-DTPA, all of the murine cell lines showed a slight increase in PD-L1 expression when compared with BV711. The highest value observed for 6E11-DTPA was in the MOPC315 cell line (79.2%), while the lowest were for LLC (26.8%) and B16F10 (20.7%).

These results indicate that MPDL3280A and 6E11 display a suitable binding towards PD-L1 expression in specific cell lines. Additionally, the results also demonstrate that the presence of the chelator DTPA did not affect the binding of the antibodies.

4.3.2 Cellular uptake studies

The cellular uptake studies were performed to evaluate the binding of the ^{111}In-labelled mAbs to specific cell lines. The human and murine cell lines which presented higher and lower expression of PD-L1 were used. Hence, for ^{111}In-MPDL3280A-DTPA, the cell lines used were H2444 and MCF7, with high and low expression of PD-L1, respectively; and for ^{111}In-6E11-DTPA, the cell lines used were MOPC315 and LLC, likewise.

Figure 4.8 shows the results of the cellular uptake in the different cell lines, at different time points (1h, 2h, 4h, 20h and 24h).

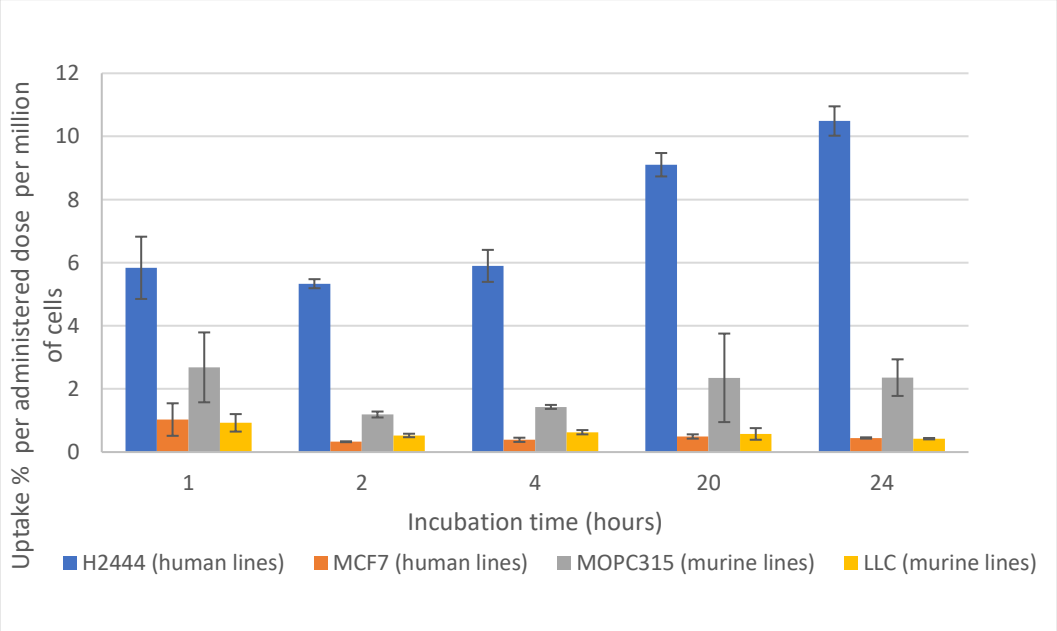

Figure 4.11. — Cellular uptake of mAbs to cell lines.

The results of the cellular uptake studies show a higher accumulation of radioactivity in the PD-L1 higher expressing cell lines compared with the lower expressing ones. ^{111}In-

MPDL3280A-DTPA displayed the highest uptake in H2444 cell lines, with 10.48% I.D./10^6 cells at 24 h post incubation. For ^{111}In-6E11-DTPA, the uptake was lower, with 2.35% I.D./10^6 cells at 24 h; however, it was still higher when compared with the low PD-L1 expressing LLC cell line (0.42% I.D./10^6 cells).

These results are in accordance with the flow cytometry studies reported above, with the higher PD-L1 expressing cell lines presenting a higher uptake of the radiolabelled mAbs, compared with the low expressing ones.

5
Conclusions and Future Work

Cancer is one of the leading causes of death worldwide. The last few years have seen major advances in the management of cancers, especially regarding targeted therapy and immunotherapy, which have changed the way this disease is now managed [116].

Immunotherapy uses a person's own immune system to fight cancer. Many monoclonal antibodies are used to treat cancer, which are designed to interact with specific targets [117]. The radiolabelling of antibodies allows for molecular imaging techniques, which are therapeutic and/or diagnostic agents in the management of cancer [118]. In this context, the aim of this work was to synthesise, radiolabel and perform preliminary biological studies for the ^{111}In radiolabelled mAbs, MPDL3280A-DTPA and 6E11-DTPA.

The mAbs, MPDL3280A and 6E11 were successfully functionalized with a DTPA derivative. QTOF-MS analysis confirmed a number of conjugated DTPA molecules ranging between 1 to 8 for MPDL3280A-DTPA; while for 6E11-DTPA the values ranged between 5 to 9.

Both DTPA-containing mAbs were radiolabelled with ^{111}In with suitable radiochemical yields and obtained with a high radiochemical purity (>95%). In vitro stability studies, in different media; NaCl 0.9%, and cell culture media DMEM and RPMI, showed that the radiolabelled mAbs were stable after 48 h of incubation.

Flow cytometry studies indicate that the mAbs are able to bind to PD-L1 expressed in specific cell lines. Particularly, MPDL3280A and MPDL3280A-DTPA displayed high PD-L1 expression in H2444 cells, while 6E11 and 6E11-DTPA showed significant expression in MOPC315 cells. Additionally, the presence of the DTPA in the mAbs does not seems to interfere with its binding capability. These results were further corroborated with the cellular uptake studies performed with the ^{111}In-labelled mAbs. ^{111}In-MPDL3280A-DTPA and ^{111}In-

6E11-DTPA displayed higher cellular accumulation in H2444 and MOPC315 cells, respectively, which had the highest expression of PD-L1.

Overall, these results demonstrate the potential of these ^{111}In-labeled mAbs for the targeting of PD-L1 expressing cancer cells.

5.1 Future Work

Although the work presented herein demonstrated promising results for these ^{111}In-labelled mAbs, further studies are still warranted, particularly by expanding on their biological evaluation. Future studies include *in vitro* blocking assays and immunoreactive fraction determination with the purpose of having a better assessment of binding of the antibodies to the PD-L1. Finally, *in vivo* biodistribution studies in mice will also be performed in order to evaluate the biological profile of the ^{111}In-labelled mAbs and the uptake in PD-L1 expressing tumors.

REFERENCES

[1] C. de Martel, D. Georges, F. Bray, J. Ferlay, and G. M. Clifford, "Global burden of cancer attributable to infections in 2018: a worldwide incidence analysis," *Lancet Glob Health*, vol. 8, no. 2, pp. e180–e190, Feb. 2020, doi: 10.1016/S2214-109X(19)30488-7.

[2] "Cancer." https://www.who.int/health-topics/cancer#tab=tab_1 (accessed Sep. 20, 2022).

[3] "Assessing national capacity for the prevention and control of noncommunicable diseases: report of the 2019 global survey." https://www.who.int/publications/i/item/9789240002319 (accessed Sep. 20, 2022).

[4] "Treatment for Cancer - NCI." https://www.cancer.gov/about-cancer/treatment (accessed Sep. 19, 2022).

[5] S. Chatterjee, W. G. Lesniak, M. Gabrielson, A. Lisok, B. Wharram, P. Sysa-Shah, B. B. Azad, M. G. Pomper, and S. Nimmagadda, "A humanized antibody for imaging immune checkpoint ligand PD-L1 expression in tumors," *Oncotarget*, vol. 7, no. 9, pp. 10215–10227, 2016, doi: 10.18632/ONCOTARGET.7143.

[6] W. G. Lesniak, S. Chartterjee, M. Gabrielson, A. Lisok, B. Wharram, M. G. Pomper, and S. Nimmagadda, "PD-L1 Detection in Tumors Using [64Cu]Atezolizumab with PET," *Bioconjug Chem*, vol. 27, no. 9, pp. 2103–2110, Sep. 2016, doi: 10.1021/ACS.BIOCONJCHEM.6B00348.

[7] E. B. Ehlerding, C. G. England, D. G. McNeel, and W. Cai, "Molecular Imaging of Immunotherapy Targets in Cancer," *Journal of Nuclear Medicine*, vol. 57, no. 10, pp. 1487–1492, Oct. 2016, doi: 10.2967/jnumed.116.177493.

[8] Y. Han, D. Liu, and L. Li, "PD-1/PD-L1 pathway: current researches in cancer.," *Am J Cancer Res*, vol. 10, no. 3, pp. 727–742, 2020.

[9] S. C. Vaz, A. S. Capacho, F. P. Oliveira, N. Gil, C. T. Barros, A. Parreira, and D. C. Costa, "Radiopharmacology and molecular imaging of PD-L1 expression in cancer," *Clin Transl Imaging*, vol. 6, no. 6, pp. 429–439, Dec. 2018, doi: 10.1007/s40336-018-0303-x.

[10] F. Bensch, E. L. Van der Veen, M. N. Lub-de Hooge, A. Jorritsma-Smit, R. Boellaard, I. C. Kok, S. F. Oosting, C. P. Schroder, T. J. N. Hiltermann, A. J van der Wekken, H. J. M. Groen, T. C. Kwee, S. G. Elias, J. A. Gietema, S. S. Bohorquez, A. de Crespigny, S. Williams, C. Mancao, A. H. Brouwers, B. M. Fine, and E. G. E de Vries, "89Zr-atezolizumab imaging as a non-invasive approach to assess clinical response to PD-L1 blockade in cancer," *Nat Med*, vol. 24, no. 12, pp. 1852–1858, Dec. 2018, doi: 10.1038/s41591-018-0255-8.

[11] H. W. Lee, T. D. Singh, S. Lee, J. Ha, A. Rehemtulla, B. Ahn, Y. H. Jeon, and J. Lee., "Evaluation of therapeutic effects of natural killer (NK) cell-based immunotherapy in mice using *in vivo* apoptosis bioimaging with a caspase-3 sensor," *The FASEB Journal*, vol. 28, no. 7, pp. 2932–2941, Jul. 2014, doi: 10.1096/fj.13-243014.

[12] C. Leten, J. Trekker, T. Struys, V. D. Roobrouck, T. Dresselaers, G. V. Velde, I. Lambrichts, C. M. Verfaillie, and U. Himmelreich, "Monitoring the Bystander Killing Effect of Human Multipotent Stem Cells for Treatment of Malignant Brain Tumors," *Stem Cells Int*, vol. 2016, pp. 1–14, 2016, doi: 10.1155/2016/4095072.

[13] H. W. Lee, P. Gangadaran, S. Kalimuthu, and B.-C. Ahn, "Advances in Molecular Imaging Strategies for *In Vivo* Tracking of Immune Cells," *Biomed Res Int*, vol. 2016, pp. 1–10, 2016, doi: 10.1155/2016/1946585.

[14] B.-C. Ahn, "Sodium Iodide Symporter for Nuclear Molecular Imaging and Gene Therapy: From Bedside to Bench and Back," *Theranostics*, vol. 2, no. 4, pp. 392–402, 2012, doi: 10.7150/thno.3722.

[15] J. Deguine, B. Breart, F. Lemaître, J. P. di Santo, and P. Bousso, "Intravital Imaging Reveals Distinct Dynamics for Natural Killer and CD8+ T Cells during Tumor Regression," *Immunity*, vol. 33, no. 4, pp. 632–644, Oct. 2010, doi: 10.1016/j.immuni.2010.09.016.

[16] E. M. Mace and J. S. Orange, "New views of the human NK cell immunological synapse: recent advances enabled by super- and high-resolution imaging techniques," *Front Immunol*, vol. 3, 2013, doi: 10.3389/fimmu.2012.00421.

[17] S. Parakh, S. T. Lee, H. K. Gan, and A. M. Scott, "Radiolabeled Antibodies for Cancer Imaging and Therapy," *Cancers (Basel)*, vol. 14, no. 6, p. 1454, Mar. 2022, doi: 10.3390/cancers14061454.

[18] "Chemical Analysis, Life Sciences, and Diagnostics | Agilent." https://www.agilent.com/en-us/PageUnavailable?s=//www.agilent.com/en/product/pharmdx/the-pd-1-pd-l1-pathway (accessed Oct. 17, 2022).

[19] "Cancer Statistics for the UK | Cancer Research UK." https://www.cancerresearchuk.org/health-professional/cancer-statistics/statistics-by-cancer- (accessed Sep. 19, 2022).

[20] S. Tan, D. Li, and X. Zhu, "Cancer immunotherapy: Pros, cons and beyond," *Biomedicine and Pharmacotherapy*, vol. 124, Apr. 2020, doi: 10.1016/J.BIOPHA.2020.109821.

[21] "What Are the Pros and Cons of Immunotherapy?" https://www.webmd.com/cancer/immunotherapy-risks-benefits#1 (accessed Sep. 20, 2022).

[22] W. G. Lesniak, S. Chartterjee, M. Gabrielson, A. Lisok, B. Wharram, M. G. Pomper, and S. Nimmagadda, "PD-L1 Detection in Tumors Using [^{64} Cu]Atezolizumab with PET," *Bioconjug Chem*, vol. 27, no. 9, pp. 2103–2110, Sep. 2016, doi: 10.1021/acs.bioconjchem.6b00348.

[23] J. R. Brahmer, S. S. Tykodi, L. Q. M. Chow, W. Hwu, S. L. Topalian, P. Hwu, C. G. Drake, L. H. Camacho, J. Kauh, K. Odunsi, H. C. Pitot, O. Hamid, S. Bhatia, R. Martins, K. Eaton, S. Chen, T. M. Salay, S. Alaparthy, J. F. Grosso, A. J. Korman, S. M. Parker, S. Agrawal, S. M. Goldberg, D. M. Pardoll, A. Gupta, and J. M. Wigginton, "Safety and Activity of Anti–PD-L1 Antibody in Patients with Advanced Cancer," *New England Journal of Medicine*, vol. 366, no. 26, pp. 2455–2465, Jun. 2012, doi: 10.1056/NEJMoa1200694.

[24] T. Powles, J. P. Eder, G. D. Fine, F. S. Braiteh, Y. Loriot, C. Cruz, J. Bellmunt, H. A. Burris, D. P. Petrylak, S. Teng, X. Shen, Z. Boyd, P. S. Hedge, D. S. Chen, and N. J. Vogelzang, "MPDL3280A (anti-PD-L1) treatment leads to clinical activity in metastatic bladder cancer," *Nature*, vol. 515, no. 7528, pp. 558–562, Nov. 2014, doi: 10.1038/nature13904.

[25] M. Hettich, F. Braun, M. D. Bartholomä, R. Schirmbeck, and G. Niedermann, "High-Resolution PET Imaging with Therapeutic Antibody-based PD-1/PD-L1 Checkpoint Tracers," *Theranostics*, vol. 6, no. 10, pp. 1629–1640, 2016, doi: 10.7150/thno.15253.

[26] D. T. Frederick, A. Piris, A. P. Cogdill, Z. A. Cooper, C. Lezcano, C. R. Ferrone, D. Mitra, A. Boni, L. P. Newton, C. Liu, W. Peng, R. J. Sullivan, S. P. Lawrence, F. S. Hodi, W. W. Overwijk, G. Lizée, G. F. Murphy, P. Hwu, K. T. Flaherty, D. E. Fisher, and J. A. Wargo, "BRAF Inhibition Is Associated with Enhanced Melanoma Antigen Expression and a More Favorable Tumor Microenvironment in Patients with Metastatic Melanoma," *Clinical Cancer Research*, vol. 19, no. 5, pp. 1225–1231, Mar. 2013, doi: 10.1158/1078-0432.CCR-12-1630.

[27] "PD L1 Monoclonal Antibody (PDL1) - Purified Mouse Monoclonal Antibody (Mab) WB, IHC-P, FC, IHC-P-Leica - Buy Now! | Abcepta." https://www.abcepta.com/products/AW5698-PD-L1-Monoclonal-Antibody-PDL1 (accessed Oct. 17, 2022).

[28] F. Kraeber-Bodere, C. Bailly, M. Chérel, and J.-F. Chatal, "ImmunoPET to help stratify patients for targeted therapies and to improve drug development," *Eur J Nucl Med Mol Imaging*, vol. 43, no. 12, pp. 2166–2168, Nov. 2016, doi: 10.1007/s00259-016-3458-6.

[29] P. N. Aguiar, L. A. Perry, J. Penny-Dimri, H. Babiker, H. Tadokoro, R. A de Mello, and G. L. Lopes Jr, "The effect of PD-L1 testing on the cost-effectiveness and economic impact of immune checkpoint inhibitors for the second-line treatment of NSCLC," *Annals of Oncology*, vol. 28, no. 9, pp. 2256–2263, Sep. 2017, doi: 10.1093/annonc/mdx305.

[30] S. Chatterjee, W. G. Lesniak, M. Gabrielson, A. Lisok, B. Wharram, P. Sysa-Shah, B. B. Azad, M. G. Pomper, and S. Nimmagadda, "A humanized antibody for imaging immune checkpoint ligand PD-L1 expression in tumors," *Oncotarget*, vol. 7, no. 9, pp. 10215–10227, Mar. 2016, doi: 10.18632/oncotarget.7143.

[31] N. J. Shah, W. J. Kelly, S. v. Liu, K. Choquette, and A. Spira, "Product review on the Anti-PD-L1 antibody atezolizumab," *Hum Vaccin Immunother*, vol. 14, no. 2, pp. 269–276, Feb. 2018, doi: 10.1080/21645515.2017.1403694.

[32] S. S. Rinne and A. Vorobyeva, "Radiometals—Chemistry and radiolabeling," *Nucl Med Mol Imaging*, pp. 95–106, Jan. 2022, doi: 10.1016/B978-0-12-822960-6.00044-2.

[33] J. Nairne, P. B. Iveson, and A. Meijer, "Imaging in Drug Development," *Prog Med Chem*, vol. 54, pp. 231–280, Jan. 2015, doi: 10.1016/BS.PMCH.2014.10.002.

[34] P. Dobosz and T. Dzieci tkowski, "The Intriguing History of Cancer Immunotherapy," *Front Immunol*, vol. 10, p. 2965, Dec. 2019, doi: 10.3389/FIMMU.2019.02965.

[35] E. F. McCarthy, "The toxins of William B. Coley and the treatment of bone and soft-tissue sarcomas.," *Iowa Orthop J*, vol. 26, pp. 154–8, 2006.

[36] A. Hoos and C. M. Britten, "The immuno-oncology framework," *Oncoimmunology*, vol. 1, no. 3, pp. 334–339, May 2012, doi: 10.4161/onci.19268.

[37] J. L. Adams, J. Smothers, R. Srinivasan, and A. Hoos, "Big opportunities for small molecules in immuno-oncology," *Nat Rev Drug Discov*, vol. 14, no. 9, pp. 603–622, Sep. 2015, doi: 10.1038/nrd4596.

[38] Y. Zhang and Z. Zhang, "The history and advances in cancer immunotherapy: understanding the characteristics of tumor-infiltrating immune cells and their therapeutic implications," *Cellular and Molecular Immunology*, vol. 17, no. 8. Springer Nature, pp. 807–821, Aug. 01, 2020. doi: 10.1038/s41423-020-0488-6.

[39] A. M. Scott, J. P. Allison, and J. D. Wolchok, "Monoclonal antibodies in cancer therapy.," *Cancer Immun*, vol. 12, p. 14, 2012.

[40] M. N. Lub-De Hooge, J. G. W. Kosterink, P. J. Perik, H. Nijnuis, L. Tran, J. Bart, A. J. H. Suurmeijer, S. de Jong, P. L. Jager, and E. G. E de Vries, "Preclinical characterisation of 111In-DTPA-trastuzumab," *Br J Pharmacol*, vol. 143, no. 1, pp. 99–106, Sep. 2004, doi: 10.1038/sj.bjp.0705915.

[41] P. J. Perik, M. N. Lu -De Hooge, J. A. Gietema, W. T. A van der Graaf, M. A. de Korte, S. Jonkman, J. G. W. Kosterink, D. J van Veldhuisen, D. T. Sleijfer, P. L. Jager, and E. G. E de Vries, "Indium-111-labeled trastuzumab scintigraphy in patients with human epidermal growth factor receptor 2-positive metastatic breast cancer," *Journal of Clinical Oncology*, vol. 24, no. 15, pp. 2276–2282, May 2006, doi: 10.1200/JCO.2005.03.8448.

[42] D. Zahavi and L. Weiner, "Monoclonal Antibodies in Cancer Therapy", doi: 10.3390/antib9030034.

[43] S. Chatterjee, W. G. Lesniak, M. Gabrielson, A. Lisok, B. Wharram, P. Sysa-Shah, B. B. Azad, M. G. Pomper, and S. Nimmagadda, "A humanized antibody for imaging immune checkpoint ligand PD-L1 expression in tumors," *Oncotarget*, vol. 7, no. 9, pp. 10215–10227, Mar. 2016, doi: 10.18632/oncotarget.7143.

[44] F. Bensch, E. L. van der Veen, M. N. Lub-de Hooge, A. Jorritsma-Smit, R. Boellaard, I. C. Kok, S. F. Oosting, C. P. Schroder, T. J. N. Hiltermann, A. J van der Wekken, H. J. M. Groen, T. C. Kwee, S. G. Elias, J. A. Gietema, S. S. Bohorquez, A. de Crespigny, S. Williams, C. Mancao, A. H. Brouwers, B. M. Fine, and E. G. E de Vries, "89Zr-atezolizumab imaging as a non-invasive approach to assess clinical response to PD-L1 blockade in cancer," *Nat Med*, vol. 24, no. 12, pp. 1852–1858, Dec. 2018, doi: 10.1038/s41591-018-0255-8.

[45] J. R. Nedrow, A. Josefsson, S. Park, S. Ranka, S. Roy, and G. Sgouros, "Imaging of programmed cell death ligand 1: Impact of protein concentration on distribution of anti-PD-L1 SPECT agents in an immunocompetent murine model of melanoma," *Journal of Nuclear Medicine*, vol. 58, no. 10, pp. 1560–1566, Oct. 2017, doi: 10.2967/jnumed.117.193268.

[46] Y.-H. Shih, C. Peng, S. Lee, P. Chiang, C. Yao, W. Lin, T. Luo, and M. Shieh, "Incetuximab as a diagnostic agent by accessible epidermal growth factor (EGF) receptor targeting in human metastatic colorectal carcinoma." [Online]. Available: www.impactjournals.com/oncotarget/

[47] A. H. Brouwers, J. E. M van Eerd, C. Frielink, E. Oosterwijk, W. J. G. Oyen, F. H. M. Corstens, and O. C. Boerman, "Optimization of Radioimmunotherapy of Renal Cell Carcinoma: Labeling of Monoclonal Antibody cG250 with 131 I, 90 Y, 177 Lu, or 186 Re."

[48] "A phase I multiple dose, dose escalation study of cG250 monoclonal antibody in patients with advanced renal cell carcinoma - PubMed." https://pubmed.ncbi.nlm.nih.gov/17705349/ (accessed Nov. 29, 2022).

[49] M. Brom, L. Joosten, W. J. Oyen, M. Gotthardt, and O. C. Boerman, "Improved labelling of DTPA-and DOTA-conjugated peptides and antibodies with 111 In in HEPES and MES buffer," 2012. [Online]. Available: http://www.ejnmmires.com/content

/2/1/4

[50] P. Laverman, T. van der Geest, S. Y. A. Terry, D. Gerrits, B. Walgreen, M. M. Helsen, T. K. Nayak, A. Freimoser-Grundschober, I. Waldhauer, R. J. Hosse, E. Moessner, P. Umana, C. Klein, W. J. G. Oyen, M. I. Koenders, and O. C. Boerman, "Immuno-PET and immuno-SPECT of rheumatoid arthritis with radiolabeled anti-fibroblast activation protein antibody correlates with severity of arthritis," *Journal of Nuclear Medicine*, vol. 56, no. 5, pp. 778–783, May 2015, doi: 10.2967/jnumed.114.152959.

[51] S. Heskamp *et al.*, "Noninvasive imaging of tumor PD-L1 expression using radiolabeled Anti-PD-L1 antibodies," *Cancer Res*, vol. 75, no. 14, pp. 2928–2936, Jul. 2015, doi: 10.1158/0008-5472.CAN-14-3477.

[52] A. Josefsson, W. Hobo, J. D. M. Molkenboer-Kuenen, D. Olive, W. J. G. Oyen, H. Dolstra, and O. C. Boerman, "Imaging, biodistribution, and dosimetry of radionuclide-labeled PD-L1 antibody in an immunocompetent mouse model of breast cancer," *Cancer Res*, vol. 76, no. 2, pp. 472–479, Jan. 2016, doi: 10.1158/0008-5472.CAN-15-2141.

[53] Y. Funase, E. Nakamura, M. Kajita, Y. Saito, S. Oshikiri, M. Kitano, M. Tokura, A. Hino, and T. Uehara, "Preclinical characterization of the radioimmunoconjugate 111In or 90Y-FF-21101 against a P-Cadherin-expressing tumor in a mouse xenograft model and a nonhuman primate," *Journal of Nuclear Medicine*, vol. 62, no. 2, pp. 232–239, Feb. 2021, doi: 10.2967/jnumed.120.245837.

[54] M. R. Lewis, J. Y. Kao, A. L. J. Anderson, J. E. Shively, and A. Raubitschek, "An improved method for conjugating monoclonal antibodies with N-hydroxysulfosuccinimidyl DOTA," *Bioconjug Chem*, vol. 12, no. 2, pp. 320–324, 2001, doi: 10.1021/bc0000886.

[55] "Technology evaluation: cT84.66, City of Hope - PubMed." https://pubmed.ncbi.nlm.nih.gov/15011786/ (accessed Nov. 29, 2022).

[56] K. E. Henry, K. N. Mak, V. L. Nagle, M. Cornejo, A. O. Michel, I. L. Fox, M. Davydova, T. R. Dilling, N. Pillarsetty, and J. S. Lewis, "ERK Inhibition Improves Anti-PD-L1 Immune Checkpoint Blockade in Preclinical Pancreatic Ductal Adenocarcinoma," *Mol Cancer Ther*, vol. 20, no. 10, pp. 2026–2034, Oct. 2021, doi: 10.1158/1535-7163.MCT-20-1112.

[57] C. Christensen, L. K. Kristensen, M. Z. Alfsen, C. H. Nielsen, and A. Kjaer, "Quantitative PET imaging of PD-L1 expression in xenograft and syngeneic tumour models using a site-specifically labelled PD-L1 antibody," *Eur J Nucl Med Mol Imaging*, vol. 47, no. 5, pp. 1302–1313, May 2020, doi: 10.1007/S00259-019-04646-4.

[58] Y. Tie, H. Yang, R. Zhao, H. Zheng, D. Yang, J. Zhao, and M. Liu, "Safety and efficacy of atezolizumab in the treatment of cancers: a systematic review and pooled-analysis," *Drug Des Devel Ther*, vol. 13, p. 523, 2019, doi: 10.2147/DDDT.S188893.

[59] R. S. Herbst, J. Soria, M. Kowanetz, G. D. Fine, O. Hamid, M. S. Gordon, J. A. Sosman, D. F. McDermott, J. D. Powderly, S. N. Gettinger, H. E. K. Kohrt, L. Horn, D. P. Lawrence, S. Rost, H. E. K. Khort, L. Horn, D. P. Lawrence, S. Rost, M. Leabman, Y. Xiao, A. Mokatrin, H. Koeppen, P. S. Hegde, I. Mellman, D. S. hen, and F. S. Hodi, "Predictive correlates of response to the anti-PD-L1 antibody MPDL3280A in cancer patients," *Nature*, vol. 515, no. 7528, p. 563, Nov. 2014, doi: 10.1038/NATURE14011.

[60] A. Aleem and H. Shah, "Atezolizumab," *Tagliche Praxis*, vol. 61, no. 3, pp. 526–532, May 2022, doi: 10.1007/s40278-022-26364-5.

[61] "Atezolizumab for Urothelial Carcinoma." [Online]. Available: http://www.fda.gov/downloads/drugs/guidancecomplianceregulatoryinformation/guidances/ucm358301.pdf

[62] N. vander Velde, A. Guerin, R. Ionescu-Ittu, S. Shi, E. Wu, S. Lin, L. Hsu, K. Saum, S. de Ducla, J. Wang, S. Lin, L. Hsu, K. Saum, S. de Ducla, J. Wang, S. Li, A. Thastrom, S. Liu, L. Shi, and J. Leppert, "Comparative Effectiveness of Non-cisplatin First-line Therapies for Metastatic Urothelial Carcinoma: Phase 2 IMvigor210 Study Versus US Patients Treated in the Veterans Health Administration," *Eur Urol Oncol*, vol. 2, no. 1, pp. 12–20, Feb. 2019, doi: 10.1016/J.EUO.2018.07.003.

[63] B. Szabados, M. Ponz-Sarvisé, R. Machado, D. Saldana, E. E. Kadel, R. Banhereau, F. Bouquet, M. Garmhausen, T. Powles, and C. Schroder, "Clinico-Genomic Characterization of Patients with Metastatic Urothelial Carcinoma in Real-World Practice Identifies a Novel Bladder Immune Performance Index (BIPI)," *Clin Cancer Res*, vol. 28, no. 18, pp. 4083–4091, Sep. 2022, doi: 10.1158/1078-0432.CCR-22-0200.

[64] "FDA approves atezolizumab as adjuvant treatment for non-small cell lung cancer | FDA." https://www.fda.gov/drugs/resources-information-approved-drugs/fda-approves-atezolizumab-adjuvant-treatment-non-small-cell-lung-cancer (accessed Dec. 13, 2022).

[65] "FDA Approves Genentech's Tecentriq in Combination With Avastin and Chemotherapy for the Initial Treatment of Metastatic Non-Squamous Non-Small Cell Lung Cancer." https://www.drugs.com/newdrugs/fda-approves-genentech-s-tecentriq-combination-avastin-chemotherapy-initial-metastatic-non-squamous-4883.html (accessed Dec. 13, 2022).

[66] "FDA Approves Atezo for ED-SCLC".

[67] T. Asco and P. Staff, "FDA Approves Atezolizumab Plus Cobimetinib/Vemurafenib for Advanced BRAF V600-Mutated Melanoma," 2020. [Online]. Available:

https://ascopost.com/issues/august-25-2020/fda-approves-atezolizumab-plus-cobimetinibvemurafenib-for-advanced-braf-v600-mutated-melanoma/1/4

[68] K. E. Henry, K. N. Mack, V. L. Nagle, M. Cornejo, A. O. Michel, I. L. Fox, M. Davydova, T. R. Dilling, N. Pillarsetty, and S. Lewis, "ERK Inhibition Improves Anti-PD-L1 Immune Checkpoint Blockade in Preclinical Pancreatic Ductal Adenocarcinoma," *Mol Cancer Ther*, vol. 20, no. 10, pp. 2026–2034, Oct. 2021, doi: 10.1158/1535-7163.MCT-20-1112.

[69] J. Zhao, X. Wen, T. Li, S. Shi, C. Xiong, Y. A. Wang, and C. Li, "Concurrent Injection of Unlabeled Antibodies Allows Positron Emission Tomography Imaging of Programmed Cell Death Ligand 1 Expression in an Orthotopic Pancreatic Tumor Model," *ACS Omega*, vol. 5, no. 15, pp. 8474–8482, Apr. 2020, doi: 10.1021/ACSOMEGA.9B03731.

[70] C. Christensen, L. K. Kristensen, M. Z. Alfsen, C. H. Nielsen, and A. Kjaer, "Quantitative PET imaging of PD-L1 expression in xenograft and syngeneic tumour models using a site-specifically labelled PD-L1 antibody," *Eur J Nucl Med Mol Imaging*, vol. 47, no. 5, pp. 1302–1313, May 2020, doi: 10.1007/S00259-019-04646-4.

[71] S. Annunziata and A. Giordano, "Nuclear medicine and immunotherapy: many questions but not many answers yet," vol. 7, pp. 3–5, 2019, doi: 10.1007/s40336-018-00312-1.

[72] J. M. Obaldo and B. E. Hertz, "The early years of nuclear medicine: A Retelling.," *Asia Ocean J Nucl Med Biol*, vol. 9, no. 2, pp. 207–219, 2021, doi: 10.22038/aojnmb.2021.55514.1385.

[73] "Ernest Rutherford | Science History Institute." https://www.sciencehistory.org/historical-profile/ernest-rutherford (accessed Jan. 25, 2023).

[74] A. M. Scott, "The State of the Art in Nuclear Medicine."

[75] "About Nuclear Medicine & Molecular Imaging - SNMMI." https://www.snmmi.org/AboutSNMMI/Content.aspx?ItemNumber=6433 (accessed Jan. 24, 2023).

[76] F. D. Rollo, "Molecular imaging: an overview and clinical applications.," *Radiol Manage*, vol. 25, no. 3, pp. 28–32; quiz 33–5, 2003.

[77] C. Xu, L. Mu, I. Roes, D. Miranda-Nieves, M. Nahrendorf, J. A. Ankrum, W. Zhao, and J. M. Karp, "Nanoparticle-based monitoring of cell therapy," *Nanotechnology*, vol. 22, no. 49, p. 494001, Dec. 2011, doi: 10.1088/0957-4484/22/49/494001.

[78] N. Institute of Biomedical Imaging, "Nuclear Medicine," 2022. [Online]. Available: www.nibib.nih.gov

[79] K. A. Wood, P. J. Hoskin, and M. I. Saunders, "Positron Emission Tomography in Oncology: A Review," *Clin Oncol*, vol. 19, no. 4, pp. 237–255, May 2007, doi: 10.1016/j.clon.2007.02.001.

[80] W. Wolf and J. Shani, "Criteria for the selection of the most desirable radionuclide for radiolabeling monoclonal antibodies," *Int J Rad Appl Instrum B*, vol. 13, no. 4, pp. 319–324, Jan. 1986, doi: 10.1016/0883-2897(86)90004-8.

[81] R. A. Fawwaz, T. S. T. Wang, S. C. Srivastava, and M. A. Hardy, "The use of radionuclides for tumor therapy," *Int J Rad Appl Instrum B*, vol. 13, no. 4, pp. 429–436, Jan. 1986, doi: 10.1016/0883-2897(86)90021-8.

[82] P. A. Schubiger, R. Alberto, and A. Smith, "Vehicles, Chelators, and Radionuclides: Choosing the 'Building Blocks' of an Effective Therapeutic Radioimmunoconjugate," *Bioconjug Chem*, vol. 7, no. 2, pp. 165–179, Jan. 1996, doi: 10.1021/bc950097s.

[83] G. Gebhart, L. E. Lamberts, Z. Wimana, C. Garcia, P. Emonts, L. Ameye, S. Stroobants, M. Huizing, P. Aftimos, J. Tol, W. J. G. Oyen, D. J. Vugts, O. S. Hoekstra, C. P. Schroder, C. W. Menke-van der Houven van Oordt, T. Guiot, A. H. Brouwers, A. Awada, E. G. E. de Vries, and P. Flamen, "Molecular imaging as a tool to investigate heterogeneity of advanced HER2-positive breast cancer and to predict patient outcome under trastuzumab emtansine (T-DM1): the ZEPHIR trial," *Annals of Oncology*, vol. 27, no. 4, pp. 619–624, Apr. 2016, doi: 10.1093/annonc/mdv577.

[84] T. Yasuda, M. D. Igor, F. Palacios, M. D. G. William Dec, J. T. Fallon, H. K. Gold, R. C. Leinbach, H. W. Strauss, B. A. Khaw, and E. Haber, "Indium lil-monoclonal antimyosin antibody imaging in the diagnosis of acute myocarditis." [Online]. Available: http://ahajournals.org

[85] "Nuclear Medicine." https://www.nibib.nih.gov/science-education/science-topics/nuclear-medicine (accessed Nov. 29, 2022).

[86] R. M. Reilly, D. A. Scollard, J. Wang, H. Mondal, P. Chen, L. Henderson, B. M. Bowen, and K. A. Vallis, "A Kit Formulated Under Good Manufacturing Practices for Labeling Human Epidermal Growth Factor with 111 In for Radiotherapeutic Applications."

[87] A. Rahmim and H. Zaidi, "PET versus SPECT: strengths, limitations and challenges," *Nucl Med Commun*, vol. 29, no. 3, pp. 193–207, Mar. 2008, doi: 10.1097/MNM.0b013e3282f3a515.

[88] V. Tolmachev, A. Orlova, and K. Andersson, "Methods for Radiolabelling of Monoclonal Antibodies," 2014, pp. 309–330. doi: 10.1007/978-1-62703-586-6_16.

[89] M. Chomet, G. A. M. S. van Dongen, and D. J. Vugts, "State of the Art in Radiolabeling of Antibodies with Common and Uncommon Radiometals for Preclinical and Clinical Immuno-PET," 2021, doi: 10.1021/acs.bioconjchem.1c00136.

[90] "chelation," in *The IUPAC Compendium of Chemical Terminology*, Research Triangle Park, NC: International Union of Pure and Applied Chemistry (IUPAC), 2014. doi: 10.1351/goldbook.C01012.

[91] J. v. Frangioni, "New Technologies for Human Cancer Imaging," *Journal of Clinical Oncology*, vol. 26, no. 24, p. 4012, Aug. 2008, doi: 10.1200/JCO.2007.14.3065.

[92] Y. Liu, G. Liu, and D. J. Hnatowich, "A brief review of chelators for radiolabeling oligomers," *Materials*, vol. 3, no. 5, pp. 3204–3217, 2010, doi: 10.3390/ma3053204.

[93] "What is a Chelating Agent? - Definition from Corrosionpedia." https://www.corrosionpedia.com/definition/254/chelating-agent (accessed Nov. 08, 2022).

[94] S. S. Rinne and A. Vorobyeva, "Radiometals—Chemistry and radiolabeling," *Nucl Med Mol Imaging*, pp. 95–106, Jan. 2022, doi: 10.1016/B978-0-12-822960-6.00044-2.

[95] B. Noll, B. Johannsen, K. May, and H. Spies, "Preparation of the renal function and imaging agent 99mTc-MAG3 starting from S-unprotected mercaptoacetyltriglycine," *Int J Rad Appl Instrum A*, vol. 43, no. 7, pp. 899–901, Jul. 1992, doi: 10.1016/0883-2889(92)90152-5.

[96] R. J. S. Duncan, P. D. Weston, and R. Wrigglesworth, "A new reagent which may be used to introduce sulfhydryl groups into proteins, and its use in the preparation of conjugates for immunoassay," *Anal Biochem*, vol. 132, no. 1, pp. 68–73, Jul. 1983, doi: 10.1016/0003-2697(83)90426-8.

[97] J. Schlesinger, J. Rajander, M. A. Avila-Rodriguez, V. Fagerholm, P. Nuutila, and O. Solin, "Radiosynthesis of New [^{90} Y]-DOTA-Based Maleimide Reagents Suitable for the Prelabeling of Thiol-Bearing <scp>l</scp> -Oligonucleotides and Peptides," *Bioconjug Chem*, vol. 20, no. 7, pp. 1340–1348, Jul. 2009, doi: 10.1021/bc900095k.

[98] L. M. de León-Rodríguez and Z. Kovacs, "The Synthesis and Chelation Chemistry of DOTA Peptide Conjugates," *Bioconjug Chem*, vol. 19, no. 2, pp. 391–402, Feb. 2008, doi: 10.1021/bc700328s.

[99] J. Schlesinger, I. Koezle, R. Bergmann, S. Tamburini, C. Bolzati, F. Tisato, B. Noll, S. Klussmann, S. Vonhoff, F. Wuest, H. Pietzsch, and J. Steinbach, "An ^{86} Y-Labeled Mirror-Image Oligonucleotide: Influence of Y-DOTA Isomers on the Biodistribution in Rats," *Bioconjug Chem*, vol. 19, no. 4, pp. 928–939, Apr. 2008, doi: 10.1021/bc700453h.

[100] G. Liu, D. Chengg, S. Dou, X. Chenm M. Liang, P. H. Pretorius, M. Rusckowski, and D. J. Hnatowich, "Replacing 99m Tc with 111 In improves MORF/cMORF pretargeting by reducing intestinal accumulation", doi: 10.1007/s11307-009-0209-0.

[101] D. J. Hnatowich, W. W. Layne, R. L. Childs, D. Lanteigne, M. A. Davis, T. W. Griffin, and P. W. Doherty, "Radioactive Labeling of Antibody: A Simple and Efficient Method," *Science (1979)*, vol. 220, no. 4597, pp. 613–615, May 1983, doi: 10.1126/science.6836304.

[102] R. L. Childs and D. J. Hnatowich, "Optimum conditions for labeling of DTPA-coupled antibodies with technetium-99m.," *J Nucl Med*, vol. 26, no. 3, pp. 293–9, Mar. 1985.

[103] L. Hassanzadeh, S. Chen, and R. N. Veedu, "Radiolabeling of Nucleic Acid Aptamers for Highly Sensitive Disease-Specific Molecular Imaging.," *Pharmaceuticals (Basel)*, vol. 11, no. 4, Oct. 2018, doi: 10.3390/ph11040106.

[104] J. Hovinen, "Labeling of Oligonucleotides with DTPA and DOTA on Solid Phase," *Nucleosides Nucleotides Nucleic Acids*, vol. 26, no. 10–12, pp. 1459–1462, Nov. 2007, doi: 10.1080/15257770701542488.

[105] R. M. Reilly, D. A. Scollard, J. Wang, H. Mondal, P. Chen, L. A. Henderson, B. M. Bowen, K. A. Vallis, "A Kit Formulated Under Good Manufacturing Practices for Labeling Human Epidermal Growth Factor with 111 In for Radiotherapeutic Applications."

[106] R. Reilly, N. Lee, S. Houle, J. Law, and A. Marks, "In vitro stability of EDTA and DTPA immunoconjugates of monoclonal antibody 2G3 labeled with indium-111," *Int J Rad Appl Instrum A*, vol. 43, no. 8, pp. 961–967, Aug. 1992, doi: 10.1016/0883-2889(92)90214-Y.

[107] "SAFETY DATA SHEET".

[108] "Amicon® Ultra-4 and -15 Centrifugal Filter Units – 10,000 NMWL – For in vitro diagnostic use (CE) - Sample Prep Centrifugal Filter Units." https://www.merckmillipore.com/PT/en/product/Amicon-Ultra-4-and-15-Centrifugal-Filter-Units-10000NMWL-For-in-vitro-diagnostic-use-CE,MM_NF-C78144?ReferrerURL=https%3A%2F%2Fwww.google.com%2F (accessed Jan. 11, 2023).

[109] "Thermo Scientific NanoDrop 2000," 2009, Accessed: Jan. 11, 2023. [Online]. Available: www.nanodrop.com

[110] A. Josefsson, J. R. Nedrow, S. Park, S. R. Banerjee, A. Rittenbach, F. Jammes, B. Tsui, G. Sgouros, "Imaging, biodistribution, and dosimetry of radionuclide-labeled PD-L1 antibody in an immunocompetent mouse model of breast cancer," *Cancer Res*, vol. 76, no. 2, p. 472, Jan. 2016, doi: 10.1158/0008-5472.CAN-15-2141.

[111] A. D'Onofrio, L. Gano, R. Melo, F. Mendes, M. C. Oliveira, T. Denoel, N. Schaefer, D. Viertl, J. Fierle, G. Coukos, S. Dunn, J. O Prior, and A. Paulo, "Biological evaluation of new TEM1 targeting recombinant antibodies for radioimmunotherapy: In vitro, in vi-

vo and in silico studies," *European Journal of Pharmaceutics and Biopharmaceutics*, vol. 158, pp. 233–244, Jan. 2021, doi: 10.1016/j.ejpb.2020.11.015.

[112] "Durval Costa | Champalimaud Foundation." https://fchampalimaud.org/research/groups/durval-costa (accessed Nov. 08, 2022).

[113] "Chemical Society Reviews,"

[114] M. S. Cooper, M. T. Ma, K. Sunassee, K. P. Shw, J. D. Williams, R. L. Paul, P. S. Donnelly, and P. J. Blower, "Comparison of (64)Cu-complexing bifunctional chelators for radioimmunoconjugation: labeling efficiency, specific activity, and in vitro/in vivo stability.," *Bioconjug Chem*, vol. 23, no. 5, pp. 1029–39, May 2012, doi: 10.1021/bc300037w.

[115] P. Thakral, S. Singla, M. P. Yadav, A. Vasisht, A. Sharma, S. K. Gupta, C. S. Bal, Snehlata, and A. Malhotra,"An approach for conjugation of (177) Lu- DOTA-SCN- Rituximab (BioSim) & its evaluation for radioimmunotherapy of relapsed & refractory B-cell non Hodgkins lymphoma patients.," *Indian J Med Res*, vol. 139, no. 4, pp. 544–54, Apr. 2014.

[116] I. A. Burney and M. S. Al-Moundhri, "Major Advances in the Treatment of Cancer: What does a Non-Oncologist need to know?," *Sultan Qaboos Univ Med J*, vol. 8, no. 2, p. 137, Jul. 2008, Accessed: Jan. 31, 2023. [Online]. Available: /pmc/articles/PMC3074830/

[117] "Monoclonal Antibodies - NCI." https://www.cancer.gov/about-cancer/treatment/types/immunotherapy/monoclonal-antibodies (accessed Jan. 31, 2023).

[118] S. Parakh, S. T. Lee, H. K. Gan, and A. M. Scott, "Radiolabeled Antibodies for Cancer Imaging and Therapy," *Cancers (Basel)*, vol. 14, no. 6, Mar. 2022, doi: 10.3390/CANCERS14061454.

NOVA SCHOOL OF SCIENCE & TECHNOLOGY

RADIOLABELLED PD-L1 INHIBITOR MONOCLONAL ANTIBODIES

2023